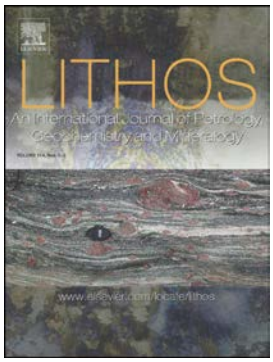

Origin of widespread cretaceous alkaline magmatism in the Central Atlantic: A single melting anomaly?

Renaud E. Merle, Fred Jourdan, Massimo Chiaradia, Hugo K.H. Olierook, Gianreto Manatschal

PII: S0024-4937(19)30238-5
DOI: https://doi.org/10.1016/j.lithos.2019.06.002
Reference: LITHOS 5098

To appear in: *LITHOS*

Received date: 25 October 2018
Accepted date: 3 June 2019" role="suppressed

Please cite this article as: R.E. Merle, F. Jourdan, M. Chiaradia, et al., Origin of widespread cretaceous alkaline magmatism in the Central Atlantic: A single melting anomaly?, LITHOS, https://doi.org/10.1016/j.lithos.2019.06.002

Origin of widespread Cretaceous alkaline magmatism in the Central Atlantic: a single melting anomaly?

Renaud E. Merle[1,*] renaud.merle@nrm.se, Fred Jourdan[2,3], Massimo Chiaradia[4], Hugo K.H. Olierook[2], Gianreto Manatschal[5]

[1]Swedish Museum of Natural History, S-104 05 Stockholm, Sweden
[2]School of Earth and Planetary Sciences, Curtin University, GPO Box U1987, Perth, WA 6845, Australia
[3]Western Australian Argon Isotope Facility & JdL Centre, Curtin University, GPO Box U1987, Perth, WA 6845, Australia
[4]Department of Earth Sciences, University of Geneva, 13 rue des Maraîchers, 1205 Geneva, Switzerland

[5]IPGS-EOST, Université de Strasbourg, 1, rue Blessig, 67084 Strasbourg, France

[*]Corresponding author.

Abstract

The age and origin of the Cretaceous magmatism on the North American and Iberian-African margins and the adjacent northern Central and Southern North Atlantic ocean are not well constrained due to the lack of appropriate data. To solve this issue, we used the $^{40}Ar/^{39}Ar$ geochronology and Sr–Nd–Pb isotopes geochemistry of basalts from the New England Seamounts and the J-Anomaly Ridge (North American margin) as these localities are still poorly investigated. We obtained a reliable age of 82.39 ± 0.12 Ma (2σ) for the Nashville Seamount (NES) and an alteration age of 76 Ma for the JAR. Our new dates from the New England Seamounts combined with those available from the Tore–Madeira Rise and SW Portugal, on the Iberia–African margins confirm an overlapping period of activity around 105–80 Ma on both the North American and Iberian-African margins and the adjacent oceanic basins. Plate kinematic reconstructions indicate that these magmatic occurrences were located within a ~1000 km radius within the yet narrow Atlantic Ocean. The J-Anomaly Ridge samples were most likely formed at the mid-Atlantic ridge around ~120 Ma.

The Sr–Nd–Pb initial isotopic ratios from the New England seamounts show similarities with the chemical signature of the Tore–Madeira Rise and, to a lesser extent, SW Portugal. Moreover, New England Seamounts display a trend towards EMI isotopic end-member, similar to those documented in at the Late Cretaceous Godzilla seamount on the Tore–Madeira Rise and sills from ODP Site 1276. The shared chemical signature is distributed across a torus-shaped area of ~2000 x 2000 km at a near-fixed location on Earth and is not temporally-controlled, suggesting a large-scale chemical anomaly in the shallow mantle. Therefore, geochronological, geochemical and plate reconstructions imply a large-scale, anomalously fertile mantle source that generated widespread magmatism during the Cretaceous in the northern Central Atlantic.

Keywords: Central Atlantic Ocean; New England Seamounts; Geochronology; Cretaceous alkaline magmatism, Tore–Madeira Rise

Introduction

The mantle plume model has been universally used to explain linear, age-progressive, intraplate oceanic magmatism (e.g. Wilson, 1963; Morgan, 1971; Coffin and Eldholm, 1994). Linear intraplate magmatic products show chemical signatures of ocean island basalts (OIB), which are attributed to the involvement of deep-rooted mantle plumes. However, not all oceanic volcanic buildings are part of alignments, nor do they necessarily show age trends that can be linked to quasi-stationary mantle plumes (Hoernle et al., 2011; Van den Bogaard et al., 2013). Demonstrating age progression along seamount chains is complicated by the difficulty in obtaining reliable ages. Moreover, pseudo-age trends may be produced when using unreliable geochronological data. For example, ages obtained using the K–Ar technique on matrix samples are very sensitive to potassium leaching during seawater alteration and do not yield reliable results for rocks older than Cenozoic (Verati and Jourdan, 2014). Nowadays, the most common method for acquiring geochronological data from volcanic seamounts is via the $^{40}Ar/^{39}Ar$ technique using mineral or groundmass separates (e.g. Verati and Jourdan, 2014). However, materials such as plagioclase or groundmass are also susceptible to K transfer during seawater alteration (Verati and Jourdan, 2014), which might prevent obtaining reliable crystallization ages. Any attempt to verify the legitimacy of age trends proposed along seamount chains has to rely on filtered datasets based on strict criteria assessing data quality (Merle et al. 2009, 2018).

The Cretaceous New England seamount (NES) chain, located off the NE US coast is probably the best example in the Atlantic Ocean of a linear seamount chain with an apparent decreasing age trend away from North America coast (Duncan, 1984; Fig. 1). Its origin has been attributed to the so-called New England hot-spot, which would include continental alkaline magmatism across the North American Plate during Jurassic and Early Cretaceous (Heaman et al., 2000). The activity of the hot-spot could have lasted up to the Late

Cretaceous to form NES, the Corner seamounts and eventually until the Miocene when it formed the Atlantis–Meteor Seamounts now located on the African Plate (Tucholke and Smoot, 1990, Sleep, 1990). However, on the oceanic sector of this hot-spot track, this hypothesis is based on unreliable geochronological and scarce isotopic data. Geochronological data for the NES chain were acquired using: (1) the K–Ar method, which is notoriously inaccurate for volcanic samples older than the Quaternary since it is not possible to test if the sample has been affected by secondary processes, (2) single-step total fusion $^{40}Ar/^{39}Ar$, which fails to provide repeat measurements from a single sample, or (3) step-heated $^{40}Ar/^{39}Ar$ measurements, which failed to yield a reliable plateau (Baksi, 2007). Moreover, most analyses were acquired on groundmass or whole-rock, in which alteration is much harder to visually detect than for mineral separates (Hofmann et al., 2000). Thus, such analysis can yield alteration-related plateau ages. In addition, no geochronological analyses exist for the Corner Seamounts and only one single age has been obtained from groundmass for the Atlantis–Meteor Seamounts (Geldmacher et al., 2006) despite previous attempts by the K-Ar method (Wendt et al., 1976). The result of combining all these data is an apparent age progression with an age distribution along the track, which seems compatible with a fixed hot-spot hypothesis (Fig. 2).

Other Late Cretaceous magmatic occurrences in the Central Atlantic Ocean and its rifted margins include the Tore–Madeira Rise (TMR) and surrounding area (Ormonde-Ampere seamounts), the J-Anomaly ridge, ODP Site 1276 alkaline sills, Newfoundland seamounts, SW Portugal (Sullivan and Keen, 1977; Tucholke and Ludwig, 1982; Geldmacher et al., 2006, Hart and Blusztajn, 2006; Grange et al., 2010; Merle et al., 2006; Miranda et al., 2009; Merle et al., 2009, 2018) and possibly the Canary Island seamount province (Van den Bogaard, 2013). Each of these provinces has been interpreted as the expression of several distinct deep mantle plumes. Such model presents the issue of the presence in a radius of

approximately 12000 km of at least five mantle plumes. Considering a head size of 1000-2000 km (Griffiths and Campbell, 1990; Campbell, 2007), this implies that these mantle plumes would be in contact with each other. This raises the question of the relevance of an alternative model involving a single melting anomaly in such a radius and at the time of the initiation of the magmatism at each of these localities. Ultimately, there is no comprehensive geodynamic model that explains the occurrence of widespread alkaline magmatism since 100 Ma in the Central Atlantic Ocean.

In this contribution, we present high quality $^{40}Ar/^{39}Ar$ ages and Sr–Nd–Pb isotopic data from the NES chain and, for the first time, from the J-Anomaly Ridge (JAR) which coincides with the J magnetic anomaly (Cretaceous). Together with a filtered database of reliable geochronological and Sr–Nd–Pb isotopic data from other Late Cretaceous alkaline magmatic products in the Central Atlantic, we test the validity of a single Late Cretaceous Central Atlantic magmatic province hypothesis. Ultimately, we assess the causes and mechanisms that facilitated magma generation and emplacement in order to form magmatic products during the Late Cretaceous in the Central Atlantic.

Geological setting

New England Seamount chain and other possibly related occurrences

The NES forms a NW–SE oriented, ~1200 km long chain of approximately 50 submarine volcanoes stretching from Bear Seamount off the coast of the NE US to the Nashville Seamount (Fig. 2). The largest edifices protrude ~3000–4000 m above the surrounding abyssal plain. All the volcanic samples recovered from the NES were altered basaltic rocks containing olivine, plagioclase and occasional primary amphibole phenocrysts (Houghton, 1979; Duncan et al., 1984). These rocks have incompatible trace and rare earth element (REE) patterns and Sr–Nd–Pb isotopic signatures typical of ocean island basalts

(OIB), which have been interpreted as compatible with a mantle plume origin (Houghton, 1979; Taras and Hart, 1987). So far, geochronological investigations on the NES volcanoes have yielded only poor-quality K–Ar, single-step $^{40}Ar/^{39}Ar$ total fusion and statistically-inconsistent step-heated $^{40}Ar/^{39}Ar$ plateau ages (Houghton et al., 1979, Duncan 1984), which can be considered unreliable from an analytical and statistical point of view (see discussion in Merle et al., 2009; Verati and Jourdan, 2014; Merle et al., 2018). Nevertheless, Duncan (1984) advocated an age progression from ~104 Ma on Bear Seamount to ~82 Ma on Nashville Seamount (Fig. 2). This trend would be compatible with the northwest-ward motion of the North America plate over a fixed mantle plume (New England hot-spot). Nevertheless, assuming a constant lithospheric drift as suggested by Duncan (1984), neighbouring seamounts such as the Atlantis II and Gosnold Seamounts show a time difference of ~9 Ma for a distance of approximately 100 km, whereas the Gosnold and Allegheny Seamounts show a time gap of ~7 Ma for a distance of 300 km, which is not compatible with a classical linear age-progression of the hot-spot track such as Hawaii (e.g. Dalrymple and Clague, 1976). This remains to be asserted with reliable geochronological investigations.

The New England hot-spot, invoked to explain the trend of the NES volcanoes, may also include the alkaline intrusions of the ~124 Ma Monteregian Hills (Foland et al., 1986) and possibly some ~124–120 Ma intrusions of the White Mountain magmatic province on inland NE Canada and US (Foland and Faul, 1977). Late Triassic to earliest Cretaceous kimberlites and other ultra-alkaline and ultramafic rocks with younger ages from west to east across Canada have been interpreted as a further continuation of the hot-spot track (e.g., Heaman et al., 2000). However, the Monteregian Hills and White Mountain intrusions might not form an alignment with the Early Triassic–earliest Cretaceous kimberlites nor with the NES (McHone, 1996). Further east of the NES, the Corner Seamounts are estimated at ~75

Ma (Tucholke and Smoot, 1990) but, to date, no expedition has collected any geological samples from these seamounts. The present-day locus of the mantle plume is now purportedly located on the Atlantis–Meteor Seamounts (Morgan, 1983, Sleep, 1990; Fig. 1). However, the Great Meteor-Atlantis seamount group have also been related to the Azores magmatic province and may not belong to the New England hot-spot track (Gente et al., 2003; Ribeiro et al., 2017). Indeed, the magmatic activity from the Atlantis–Meteor Seamounts may be more recent, ranging between 33 Ma (Plato Seamount: 33.4 ± 0.5 Ma obtained by K-Ar technique on matrix, Ribeiro et al., 2017) and 17 Ma (Great Meteor Seamount: 17.3 ± 0.3 Ma obtained by step-heating $^{40}Ar/^{39}Ar$ on matrix; Geldmacher et al., 2006). It should be noted that the dated sample from Plato Seamount presents a Loss On Ignition (LOI) of 2.5 wt% (Ribeiro et al., 2017) that does not preclude slight seawater alteration then a possible bias on the calculated age.

J-Anomaly Ridge

The JAR, located approximately 800 km to the northeast of the Nashville Seamount, is a ~1000 m high, NE–SW oriented submarine rise that extends off the south-eastern end of Grand Banks, Canada (Fig. 1). The JAR overlies the J magnetic anomaly (M3-M0 Cretaceous magnetic anomalies: 130-125 Ma; Gradstein et al., 2004), which suggests that it has been emplaced close to or at the spreading axis and has the age as the underlying oceanic crust (Tucholke and Ludwig, 1982). It was interpreted as a locally thickened oceanic crust formed together with the conjugate TMR during the final breakup of the Newfoundland–Iberia continental lithosphere (Tucholke and Ludwig, 1982). The excess magma needed to form a ridge as large as the JAR–TMR ridge requires involvement of an anomalously hot source underneath the rift axis, commonly attributed to a mantle plume (Tucholke and Ludwig, 1982). When oceanic spreading began, the newly formed ridge was split apart, forming the

JAR on the Newfoundland margin and the TMR on the Iberia margin, the latter being covered by Late Cretaceous magmatism (Tucholke and Ludwig, 1982).

The only basaltic samples recovered from the JAR were drilled during DSDP Leg 43 at Site 384 (Tucholke et al., 1979). Approximately 300 m thick marine sediments overlie directly the basalts and are interpreted as deposited between upper Barremian to lower Aptian (130-112 Ma; Tucholke et al., 1979).

The drilled rocks correspond to fine-grained basalts with common pyroxene and rare plagioclase phenocrysts. These rocks experienced various degrees of alteration by seawater, as expressed by calcite- and clay mineral-filled vesicles, patches of bowlingite (olivine alteration product), altered groundmass as well as chlorite and epidote (Houghton, 1979).

The few analysed samples display slightly enriched incompatible element patterns compared to those of normal mid-ocean ridge basalt (MORB). So far, there are no Sr–Nd–Pb isotopic data from the JAR. The few samples investigated for geochronology yielded broadly Cretaceous ages but correspond to statistically-inconsistent $^{40}Ar/^{39}Ar$ and K-Ar age data (Houghton et al., 1979).

Magmatic occurrences in the northern Central Atlantic and southern northern Atlantic area

Other OIB-like magmatic occurrences are present on the North American Plate within a radius of ~1000 km. These include two basaltic sills drilled at ODP Site 1276 (Fig. 1), which yielded a series of whole-rock $^{40}Ar/^{39}Ar$ ages of 105.3 ± 1.2 Ma and 99.7 ± 1.8 Ma for the upper and lower sills, respectively (Hart and Blusztajn, 2006). Note that the younger age from the lower sill was derived from a mini-plateau (63% of ^{39}Ar released, fully developed plateau should have more than 70% of ^{39}Ar released; Merle et al., 2009). Thus, the age may be considered as inaccurate and is likely contemporaneous with the ~105 Ma sill. These sills are located in the vicinity of the Newfoundland seamounts (Fig. 1) for which an age of ~98

Ma has been estimated based on $^{40}Ar/^{39}Ar$ measurements (Sullivan and Keen, 1977). So far, there are no ages available for the Milne seamounts (Fig. 1).

On the Iberia and Africa plates, the Cretaceous magmatic occurrences include the continental intrusions of SW Portugal (94-68 Ma), the TMR and surrounding seamounts (104-0 Ma) with the Madeira archipelago at its southern extremity (Fig. 1). These occurrences have been interpreted as the result of the activity of a deep Hawaiian-like fixed mantle plume based on an observed NE–SW age trend (Geldmacher et al., 2000; D'Oriano et al., 2010). In this model, a 450 km-wide Madeira hot-spot track imprints its path through the Iberia plate forming successively Serra de Monchique (76–68 Ma), Ormonde (66–62 Ma), Ampere (32 Ma), Unicorn (28 Ma), and Seine (22–25 Ma) seamounts and eventually the Madeira archipelago (Geldmacher et al., 2000; D'Oriano et al., 2010). A variant of this model involves the successive activities of Canary and Madeira hot-spots where TMR is built up by two magmatic phases, the first one during Cretaceous times (>95–80 Ma) related to the Canary mantle plume and the second magmatic activity (16–0.5 Ma) related to the Madeira mantle plume (Gelmacher et al., 2006). These hypotheses are poorly constrained as they rely on a partial dataset and unreliable dates (Merle et al., 2009; 2018).

It should be noted that the magmatic activity of the Canary Island seamount province (CISP) might have started as early as 142 Ma, Van den Bogaard, 2013). This suggests that the magmatic activity of the CISP could have been coeval to those of the other Cretaceous magmatic provinces in northern Central Atlantic. However, the beginning of this phase of activity is not well constrained. Indeed, many dates are unreliable as they are either weighted average ages of multiple single-step total fusion Ar measurements in plagioclase or whole-rock $^{40}Ar/^{39}Ar$ step heating technique yielding mini-plateaus (Van den Bogaard, 2013). The approach of calculating weighted average ages from multiple aliquots of single-step total fusion Ar measurements in plagioclase is not reliable as (1) plagioclase doesn't have enough

Ar to generate a proper age at the single grain level and (2) this approach is likely prone to mask any disturbance in the K/Ar system.

Based on the approximate periods of the magmatic activities on the Iberia and North America plates between 104 and 80 Ma, Merle et al. (2009) noted that all these magmatic occurrences were close to each other (~1000 km) as the Atlantic ocean was still narrow and therefore may have formed a single magmatic province. This hypothesis has not been properly tested so far.

Samples and Results

The NES samples studied here were drilled during DSDP Leg 43 at the foot of Nashville (Site 382) and Vogel seamounts (Site 385), while the JAR samples were collected on the top of the ridge at the DSDP Site 384 (see Fig. 2). The tops of DSDP Sites 382 and 385 are located 5527 m and 4956 m below sea level, respectively (Tucholke and Vogt, 1979). From these sites, only breccias containing volcanic clasts were drilled. DSDP Site 384 is located 3910 m below sea level and yielded basaltic rocks. The samples studied here were extracted from the same cores as the samples investigated by Houghton (1979). Our samples were selected at different depths along the cores and are distinct from the samples investigated by Houghton (1979). The details of sampling sites, the position of the selected rocks in the recovered cores and hand specimen descriptions are given in Table A1 in the supplementary material.

We investigated five basaltic samples from the NES and three from the JAR for $^{40}Ar/^{39}Ar$ geochronology, major and trace element contents, and Sr–Nd–Pb (method descriptions and tables including full data set of $^{40}Ar/^{39}Ar$ measurements are available in the supplementary material).

Brief Petrographic description of the investigated samples

The NES samples (NES 2, 3, 7, 8, 9 and 10; see Table A 1 in supplementary material) are breccias containing basaltic clasts of up to 5cm large cemented by calcite (Fig. 3a). Most of the clasts show a red-brown colour typical of seawater alteration (Fig. 3a-d). Some clasts are very vesicular with most of the voids filled with calcite (Fig. 3b). Phenocrysts of 2-3 mm black prismatic pyroxenes or amphiboles as well as completely oxidized olivine are visible (Fig. 3c). Other clasts are more massive with empty vesicles (Fig. 3d). The JAR samples (JAR4, 5 and 6; Table A1 in supplementary material) display a green colour and large vesicles filled with green and white alteration material. No phenocrysts are visible (Fig. 3e).

In thin sections, the porphyritic NES samples contain relatively fresh ~ 2-3mm euhedral amphibole and pyroxene phenocrystals embedded into an altered fine-grained groundmass containing very altered plagioclase microliths and glass partly transformed into clay and hydroxides (Fig. 4a, b, c). The aphyric NES samples like NES7 show a groundmass formed by ~100µm plagioclase microliths and oxides (Fg. 4d). The interstitial glass is partly transformed into hydroxides and clay (Fig. 4d).

The JAR samples show olivine phenocrysts (2% vol.) up to ~2mm in size (Fig. 4e) and transformed into bowlingite that is a green-colour alteration product of olivine (Fig. 4f). These phenocrysts are included into a groundmass formed by plagioclase laths. Vesicles are lined with hydroxides, clay and calcite (Fig. 4e).

$^{40}Ar/^{39}Ar$ dating

Six samples were dated including two hornblende separates and one groundmass fraction from the Nashville Seamount, one groundmass fraction from the Vogel Seamount and two groundmass fractions from JAR (Fig. 5). A summary of the $^{40}Ar/^{39}Ar$ data is presented in Table 1. The details of the analytical results are given in the supplementary

material. The hornblende fractions yielded two reliable plateau ages of 82.39 ± 0.12 Ma (Mean Square Weighted Deviation: MSWD = 0.24, Probability of fit: P = 1; sample NES2) and 82.25 ± 0.16 Ma (MSWD = 0.70, P = 0.81; sample NES3) that are identical within analytical uncertainties. A groundmass aliquot extracted from the sample NES3 yielded a statistically valid plateau age of 77.80 ± 0.29 Ma (MSWD = 0.28, P = 0.99) that is significantly younger (~4 Ma) than the hornblende age. Only one groundmass fraction from JAR (sample JAR6) yielded a valid plateau age of 75.96 ± 0.72 Ma (MSWD = 1.14, P = 0.33). The other two samples (NES7 and JAR5) failed to yield plateau ages (Fig. 5).

Major and trace elements

The NES samples are altered with LOI (Loss On Ignition) higher than 6.5 wt%, except one sample from the Vogel seamount (NES7, LOI = 0.78 wt%; Table A2 in supplementary material). The JAR samples are less altered according to their LOI (2.6–3.9 wt%). All the samples investigated here show evidence of interaction with seawater (see discussion of the effects of alteration on chemistry of the samples in supplementary material). In this study, we will therefore avoid using elements that are typically mobile during seawater alteration (e.g., Mg, Na, K, Ba and Sr; Pearce et al., 2008). As a consequence, the classification of the rocks using the TAS diagram (Total Alkali Silica: SiO_2 *vs.* K_2O+Na_2O) is not possible.

Despite the pervasive alteration that affected the samples (see discussion of the effects of alteration on chemistry of the samples in supplementary material), the rocks display magmatic chemical characteristics for most of the incompatible elements (IE) in particular, the high field strength elements. We plotted the NES and JAR in discriminant plots for geodynamic settings using immobile elements such as Zr, Y, Nb, Ta, Th and Yb. Specifically, we used the ternary plot Nb-Zr-Y (Meschede, 1986; Fig. 6a), Ta/Yb *vs.* Th/Yb

(Fig. 6b; modified from Pearce, 1982) and Zr *vs.* Zr/Y (Fig. 6c; Pearce and Norry, 1979). In these diagrams, the NES samples plot in the field of the OIB (within plate volcanism; Fig. 6). On the other hand, the JAR samples plot in the field or very close to the field of the MORBs (in the field of OIB, Fig. 6). Note that JAR6 plots away from the two other JAR samples in the Ta/Yb *vs.* Th/Yb and Zr *vs.* Zr/Y plots (Fig. 6b, c).

The JAR samples are near-primitive as shown by the compatible trace element contents: Co = 38–41 ppm, Ni = 144–197 ppm and Cr = 422–557 ppm. Note that JAR6 has the highest SiO_2 and highest $Fe_2O_{3(tot)}$ contents and lowest MgO, Ni and Cr contents (see Table A2 in supplementary material). However, these chemical contents are only marginally different from those of the two other JAR samples.

Immobile incompatible elements and REE patterns of the NES samples are similar to those of average OIB (Fig. 7a, b), showing enrichment in the most incompatible elements relative to the less incompatible elements. The NES samples display enriched REE patterns with $[La/Sm]_{CN}$ = 2.8–3.9 and $[Dy/Yb]_{CN}$ = 1.5–2.2 (CN: chondrite normalised ratio using the values of Sun and McDonough, 1989; Fig. 7a). The IE patterns show negative Pb and positive Nb and Ta anomalies that are typical of mantle-derived magmas uncontaminated by continental crust (Fig. 7c). The patterns of the samples investigated here overlap the field of the previously analysed samples (Houghton, 1978; Taras and Hart, 1987).

Compared to the NES, the JAR samples display distinct IE and REE patterns (Fig. 7). Two samples (JAR4 and JAR5) display IE and REE patterns similar to normal MORB (N-MORB) while the third one (JAR 6) has patterns more similar to enriched MORB (E-MORB). All the samples display slight negative Sr anomalies and positive Ta anomalies, indicating the absence of any continental crust contamination (Figs. 7b and d). Samples JAR4 and JAR5 show IE and REE patterns parallel to N-MORB with a typical depletion in light REE ($[La/Sm]_{CN}$ = 0.80–0.90) and nearly flat heavy REE pattern ($[Dy/Yb]_{CN}$ = 1.3–1.4).

Both IE and REE patterns of these two samples overlap the field of the JAR samples previously documented (Houghton, 1979). The third sample (JAR6) is more enriched in incompatible elements compared to JAR4 and JAR5 (Fig. 7b and d). It also shows an enrichment in light REE ($[La/Sm]_{CN} = 2$) and flat heavy REE pattern ($[Dy/Yb]_{CN} = 1.2$). The REE pattern of this sample is parallel to those of E-MORB (Fig. 7b). The REE pattern of JAR6 shows a significant Eu negative anomaly that is neither observed in the patterns of the two new JAR samples investigated here nor documented in previously published JAR samples (Fig. 4; Houghton, 1979). In addition, the heavy REE (Dy-Lu) and less incompatible element patterns of this sample are rather parallel to those of the other JAR samples (Fig. 7b and d).

In the JAR samples, Pb contents were below detection limit; U contents range from 0.2 to 0.8 ppm and Th contents 0.4 to 6.5 ppm with the highest concentrations measured in sample JAR6 (see Table A2 in supplementary material). This range of contents is similar to those expected for average E-MORB (Sun and McDonough, 1989) excepting for the high Th content in JAR6 which might be related to an analytical problem.

Sr–Nd–Pb isotopes

Here we present Sr-Nd-Pb isotopic data for the NES and, for the first time, for the JAR samples. The measured Sr-Nd-Pb isotopic ratios of samples were back-calculated to initial, using an age of 82 Ma from Nashville Seamount (Fig. 5) and 91 Ma for Vogel Seamount (Houghton, 1979). The measured Sr-Nd isotopic ratios of the JAR samples were back-calculated to initials using an age of 76 Ma (Fig. 5). As Pb concentrations for these samples were below detection limit and no previously published Pb elemental contents are available, the Pb isotopic data of the JAR samples were not back-calculated to initial isotopic ratios.

The NES and the JAR samples define distinct fields in the isotopic plots: the JAR plot close or in the field of the Atlantic MORBs while the NES plot in the field of OIBs (figs. 8 and 9).

For the NES samples, the initial ratios show significant variations: $^{87}Sr/^{86}Sr$ = 0.702923–0.704683; $^{143}Nd/^{144}Nd$ = 0.512757–0.512823; $^{206}Pb/^{204}Pb$ = 19.14–20.36; $^{207}Pb/^{204}Pb$ = 15.55–16.09; $^{208}Pb/^{204}Pb$ = 38.71–40.342 (Figs. 8 and 9). In some samples, Pb and Sr isotopic ratios are considered unreliable. For instance, the highest $^{207}Pb/^{204}Pb$ isotopic ratio from NES 7 (Vogel) is anomalously high (16.09) and clearly distinct from the Pb isotopic ratios observed in the all other NES samples (Table 2). Therefore, this ratio is considered suspicious and will not be considered any further. However, the other Pb isotopic ratios for this sample are not very different from those observed in the other NES samples. They do not show any evidence of analytical issues and are considered reliable. $^{87}Sr/^{86}Sr$ initial ratios are correlated with LOI in the NES samples (Fig. A2 in supplementary material). This is a common phenomenon in submarine samples due the mobility of Sr during seawater alteration as shown by the trend of decreasing Sr content with increasing LOI (Fig. A2 in supplementary material). Note that such a correlation is not observed for the Pb isotopic ratios (Fig. A2 in supplementary material). Only initial $^{87}Sr/^{86}Sr$ ratio obtained from sample NES7 ($^{87}Sr/^{86}Sr$ = 0.702923), which has the lowest LOI (0.78 %) can be considered reliable. We therefore omit the $^{207}Pb/^{204}Pb$ isotopic ratio of NES7 and the Sr isotopic ratios from all samples other than NES7 from further discussion.

In the $^{207}Pb/^{204}Pb$ *vs.* $^{206}Pb/^{204}Pb$ and $^{208}Pb/^{204}Pb$ *vs.* $^{206}Pb/^{204}Pb$ plots, the initial Pb ratios of the NES samples overlap the field defined by the previously published data of NES (Fig. 9). Like some previously published data, the data points of some samples analysed in this study straddle the Northern Hemisphere Regression Line (NHRL, Hart, 1984),; Fig. 6;) toward an HIMU-like component (High time-integrated $^{238}U/^{204}Pb$ ratio) that would be

located below this line (Fig. 9). The previously published and new NES data overlap with or are proximal to the TMR lavas, SW Portugal rocks and Great Meteor Seamount isotopic data (Fig. 9). In the $^{206}Pb/^{204}Pb$ *vs*. $^{143}Nd/^{144}Nd$ plot (Fig. 8b), the NES, ODP Site 1276 sills and Godzilla Seamount form an array between TMR and Enriched Mantle I (EMI). In particular, the lavas from Godzilla Seamount show Nd and Pb compositions close to the EMI end-member (Geldmacher et al. 2008).

For the JAR, the initial $^{87}Sr/^{86}Sr$ (0.703291–0.703438) and $^{143}Nd/^{144}Nd$ (0.512984–0.513012) and measured Pb ratios ($^{206}Pb/^{204}Pb$ = 18.165–18.418; $^{207}Pb/^{204}Pb$ = 15.432–15.522; $^{208}Pb/^{204}Pb$ = 37.861–38.094) show limited variability. In the $^{143}Nd/^{144}Nd$ *vs*. $^{87}Sr/^{86}Sr$ plot, the JAR samples plot in the field of the 0-55 °N Atlantic MORB (Fig. 8a). Sample JAR6 has IE and REE contents distinct from the two other JAR samples, has $^{87}Sr/^{86}Sr$ initial ratios overlapping within uncertainty of one of the two other samples but has higher $^{143}Nd/^{144}Nd$ initial ratios. The measured Pb ratios of the JAR samples plot in the field of the Atlantic MORB (Fig. 6). Despite these ratios being uncorrected, the effects of in-situ decay correction would not exceed 10% of the measured ratios for younger than 100 Ma assuming an E-MORB composition (Pb = 0.6 ppm, U = 0.2 ppm and Th = 0.6 ppm; Sun and McDonough, 1989). Therefore, the expected initial ratios would not differ significantly enough to move the data points out of the MORB field.

It should be noted that there is no correlation between $^{206}Pb/^{204}Pb$ or $^{87}Sr/^{86}Sr$ ratios and MgO content for the NES or JAR samples suggesting that contamination by upper continental crust did not occur (Fig. A3). In addition, this magmatism occurred on oceanic lithosphere (Louden et al., 2004). This suggests that the observed isotopic characteristics of the samples record mantle source signature.

Discussion

Our new data from both NES and JAR provide new constrains on the geodynamical triggering of the magmatic activity during Cretaceous time in the northern Central Atlantic and allow testing the single magmatic province hypothesis (Merle et al., 2009). In particular, the location of NES and JAR samples are clearly distinct in the Nb-Zr-Y, Ta/Yb *vs.* Th/Yb and Zr *vs.* Zr/Y classification diagrams with the NES having an OIB affinity while the JAR have a MORB affinity despite some enriched chemical characteristics. As NES and JAR magmatic events do not have the same age (>82 Ma for the former and ~76 Ma for the latter), it is clear that these magmatic occurrences are not genetically related.

Interpretation of age, geochemical and isotopic data of the NES and JAR

Age of the New England Seamount chain.

We obtained two statistically indistinguishable hornblende plateau ages of 82.39 ± 0.12 Ma and 82.25 ± 0.16 Ma on the Nashville seamount. Since samples NES2 and NES3 have indistinguishable ages, we calculate a weighted mean age of 82.34 ± 0.10 Ma (2σ; MSWD = 2, P = 0.16) for the age of the magmatic activity at the southern extremity of the NES chain.

Statistically reliable hornblende and groundmass ages from NES3 yielded ages that do not overlap within uncertainty. The groundmass from NES3 yielded a plateau age of 77.80 ± 0.29 Ma, ~4–5 Myr (~5.5%) younger than the hornblende age (Fig. 5). Such a discrepancy between analytically and statistically valid $^{40}Ar/^{39}Ar$ plateau ages obtained on groundmass and separated minerals has been previously observed for mafic samples, with the groundmass dates consistently younger than the ages obtained on mineral separates (see comparison between groundmass and mineral separate $^{40}Ar/^{39}Ar$ results in Hofmann et al., 2000 and Jourdan et al., 2007; Renne et al., 2015). For example, a basalt dredged on Seine Seamount

from the TMR yielded a groundmass analysis of 22.2 ± 0.2 Ma that is ~ 10% younger than the age of 24.6 ± 0.45 Ma obtained from hornblende analyses (Merle et al., 2009; 2018). It should be noted that in some case, the date yielded by the groundmass can be older than those obtained in the fresh feldspars from the same rock (Deccan basalt; Renne et al., 2015). Potassium is notorious for being mobile during rock–seawater interaction in oceanic settings (e.g. Cann, 1979; Honnorez, 1981) that can adversely affect the K-Ar geochronometer. As the groundmass has significantly more surface area than mineral phenocrysts and minerals can be more efficiently screened for alteration, mineral separates tend to retain true geochronological information while a slight alteration of the groundmass can yield apparent younger ages, which should be treated with caution and used as a minimum age for the crystallisation of the rock.

With this observation in mind, critical evaluation of published geochronological data from the NES clearly indicate that many reported ages do not conform to stringent reliability tests, including failing statistical tests (i.e., p-value indicating scatter beyond analytical uncertainties) or obtained as a single datum that prohibits verification of closed system behaviour (single step-total fusion $^{40}Ar/^{39}Ar$ and K-Ar analyses, see Baksi, 2007; Merle et al., 2009, 2018; Verati and Jourdan, 2014, for a review of critical parameters used to assess the data quality; Fig. 10). By following these strict criteria, none of the previously obtained ages on NES were found to be reliable except our hornblende separates at 82.34 ± 0.10 Ma (Fig. 5). However, the $^{40}Ar/^{39}Ar$ groundmass ages and the amphibole age with poor-statistical parameters (See age compilation in supplementary material) can provide a reasonable estimate within a few million years of the true crystallisation age of the rocks. These data can be used as semi-quantitative information to estimate the approximate period of activity of the NES. By discarding the unreliable single step-total fusion $^{40}Ar/^{39}Ar$ and K/Ar data, only eight data over twenty-eight remain to assess the timing of the magmatic activity on the NES (Fig.

10a). The filtered data form a spread between 104 and 77 Ma suggesting an intense period of magmatic activity in the Late Cretaceous on the NES (Fig. 10) but this has still to be confirmed due to the limited number of data.

The remaining data tend to display an apparent age trend (Fig. 10) which should be considered with caution: (1) only half of the seamounts previously investigated are represented in this age trend, (2) the oldest data are matrix analyses then should be considered as minimum age estimates and as such, they are still not reliable enough to establish the occurrence of an unequivocal age trend, and (3) the scatter observed among the data precludes the calculation of a statistically robust migration rate for the magmatic activity.

This latter aspect is particularly critical for the geodynamic and absolute plate reconstruction models. Indeed, many studies utilise the radio-isotopic ages from the NES as a framework for absolute plate motions (e.g., Doubrovine et al., 2012; O'Neill et al., 2005; Seton et al., 2012; Steinberger, 2000; Steinberger et al., 2004). These models may require some readjusting to accommodate the significant uncertainty on the magmatic activity migration rate.

Therefore, the apparent age trend displayed by the NES is poorly constrained and not well supported by data. As a result, there is no unambiguous age-progressive trend along the New England Seamounts chain as previously proposed (Duncan, 1984). Despite age differences might exist between the seamounts, it is difficult to assess their extent considering the potential age shift due to the seawater alteration. This illustrates the drawbacks of establishing hot-spot tracks based only on apparent age trends relying on unreliable and partial set of data.

Age and origin of the J-Anomaly Ridge

Our new plateau age of 76.0 ± 0.7 Ma obtained on JAR basaltic sample has to be interpreted with care since it was obtained on groundmass (see discussion above). Since in basaltic samples, in particular MORB, potassium is mainly incorporated into the groundmass, slight pervasive alteration could have biased the age even if the rock displays low LOI (Caroff et al., 1995; Merle et al., 2009). The sample shows a LOI slightly high for a fresh MORB (2.6%) and the petrographic evidence for seawater alteration (presence of clay minerals, chlorite and epidote, Houghton, 1979) suggests that our new age does not represent the crystallisation of the rock. Therefore, the meaning of this age has to be assessed. The JAR samples show a MORB affinity that suggests an origin related to the Mid Atlantic Ridge. South of the Newfoundland–Azores fracture zone, the area surrounding the JAR is interpreted as oceanic lithosphere (Nirrengarten et al., 2017, 2018). Specifically, the JAR overlaps the M0 magnetic anomaly, which is clearly identified in this area (Fig. 1) and has an age of ~120 Ma (Nirrengarten et al., 2017, 2018) suggesting that the JAR was formed at the same time. The first sediments overlaying the JAR have been interpreted as deposited during the Upper Barremian to lower Aptian (130–112 Ma; Tucholke et al., 1979) which argues also for an age of around 120 Ma. As the JAR samples show evidence of seawater interaction and moderate hydrothermal alteration as shown by the presence of chlorite and epidote, our age of 76.0 ± 0.7 Ma represents the age of a low-temperature alteration or hydrothermal event after the formation of the oceanic crust that occurred at 120 Ma. It is important to note that a statistically reliable groundmass mini-plateau or plateau age can thus be shifted by ~45 Ma from its true crystallization age. Therefore, it seems difficult to relate the magmatic activity on the JAR with those occurring on the TMR as suggested by previous studies (e.g. Tucholke and Ludwig, 1982). As the JAR samples tend to show a MORB-like chemical affinity (Figs. 6, 8a and 9), we conclude that these samples are originated from the local oceanic crust formed by the mid-Atlantic ridge around 120 Ma and eventually hydrothermally altered at

low temperature around 76 Ma, which is also supported by the occurrence of upper Barremian to lower Aptian sediments overlaying these basalts.

As the origin of the JAR should be related to the activity of the Mid Atlantic Ridge, this raises the issue of the origin of the geochemical characteristics of one of the JAR samples (JAR6), which is different from typical normal MORB (Fig. 7). JAR6 is only marginally different from the two other JAR samples in term of major and compatible trace elements composition (see table A2 in supplementary material). . Therefore, it seems that JAR6 is not significantly more differentiated than the other two JAR samples. JAR6 has higher middle and heavy REE contents than JAR4 and JAR5, yielding parallel Gd–Lu patterns that could be related to a more differentiated stage for JAR6 through fractional crystallisation, which could also explain the negative Eu anomaly. Nevertheless, fractional crystallisation does not explain the light REE enrichment observed specifically for this sample. The difference in terms of isotopic composition between JAR6 and the two samples is noticeable limited (Fig. 8, 9). The Sr–Nd signatures of all the JAR samples ($^{86}Sr/^{87}Sr_i$ = 0.703291–0703438; $^{143}Nd/^{144}Nd_i$ = 0512984–0.513012) are similar to those of the MORB produced by the MAR on an area located north of the Oceanographer Fracture Zone ($^{86}Sr/^{87}Sr$ = 0.703176–0.704040; $^{143}Nd/^{144}Nd$ = 0.512668–0.512992; Dosso et al., 1999). The specific chemical characteristics of these MORB, which also have high LREE contents (La/Sm >2), have been interpreted as originated from a continental lithospheric-like chemical heterogeneity in the upper mantle (Dosso et al., 1999). As the JAR basalts were formed by the Mid-Atlantic ridge in the vicinity of the Oceanographer Fracture Zone and they display isotopic characteristics similar to those of the MORBs investigated by Dosso et al. (1999), we interpret the JAR basalts as their older equivalents. The JAR would sample the same mantle source, that is, the ambient asthenosphere containing a continental-like heterogeneity. In this hypothesis, the light REE enrichment observed in the chemical characteristics of JAR6 could be related to a

stronger contribution of this shallow mantle heterogeneity compared to the other JAR samples. A shallow mantle source is also supported by the nearly flat HREE patterns of these rocks, such a feature precluding residual garnet in the source. It should be noted that the Azores mantle plume has been suggested as an origin of the enriched composition of the MORBs from the northern Oceanographer Fracture Zone area (Ribeiro et al., 2017 and references therein). We note that the postulated beginning of the Azores hot-spot activity is estimated at ~85 Ma based on the assumed age of the Corner seamount and that the main phase of magmatic activity of the Azores province started between 30-20 Ma (Gente et al., 2003; Ribeiro et al., 2017). Regardless of these poor geochronological constraints on the beginning of the Azores mantle plume activity (K–Ar dates on matrix for the Azores magmatic province and no geochronological data for Corner seamounts), the JAR was formed by the MAR at ~120 Ma implying a gap of approximately 35 Ma between this magmatic event and the very first evidence of the Azores mantle plume activity. Therefore, we suggest that the enriched signature observed in JAR6 was in the shallow asthenospheric mantle at 120 Ma and cannot be related to the Azores mantle plume.

Evidence for widespread Late Cretaceous alkaline magmatic activity in the northern Central Atlantic and southern North Atlantic

New and published geochronological, geochemical, Sr–Nd–Pb isotopic data (Figs. 8, 9 and 11) and plate reconstructions (Fig. 12) permit a re-evaluation of whether the northern Central Atlantic and southern North Atlantic alkaline magmatic occurrences form a single province (Merle et al., 2009).

In the Late Cretaceous, magmatic activity potentially coeval with the NES is occurring throughout the northern Central Atlantic and southern northern Atlantic area (Fig.

1). On the North American Plate, these include the ~80–76 Ma Corner Seamounts (Tucholke and Smoot, 1990), the ~98 Ma Newfoundland Seamounts (Sullivan and Keen, 1977) and two sills drilled close to the Newfoundland Seamounts during ODP Site 1276 (~105–100 Ma, Hart and Blusztajn, 2006). On the Iberian and African Plates, magmatic activity occurred in SW Portugal (88–68 Ma, Miranda et al., 2009; Grange et al., 2010), in the TMR and surrounding areas (103 Ma–present, Geldmacher et al., 2000, 2005, 2006, 2008; Merle et al., 2006, 2009, 2018), and in the CISP (142 Ma to present; Van den Bogaard, 2013).

It should be noted that the CISP could also have been active as early as the Early Cretaceous (142Ma; van den Bogaard 2013). However, many dates from seamounts of this province including the oldest date were obtained by either Ar total fusion (Bisabuelas seamount: ~142 Ma) or mini-plateau $^{40}Ar/^{39}Ar$ step-heating methods (Van den Bogaard, 2013). Based upon the data quality criteria already mentioned earlier, these data cannot be considered as reliable. So far the oldest reliable date is 126.3 ± 0.3 Ma obtained by step-heating on K-feldspar, which developed a full Ar degassing plateau (Klügel et al. 2011). Nevertheless, a major phase of magmatic activity occurred during the Cretaceous (>70 Ma) on the CISP and on the TMR province and lasted until the last million years despite. a gap of magmatic activity on TMR between 62 Ma and 32 Ma (Merle et al., 2018).

The chemical and isotopic characteristics of the rocks from SW Portugal, TMR and surrounding seamounts (Ormonde–Ampere), NES and ODP Site 1276 show that these Cretaceous alkaline magmatic products are derived from a depleted asthenosphere (Atlantic MORB), an EMI-like component as well as an HIMU-like component, which is required to explain the high $^{206}Pb/^{204}Pb$ and $^{208}Pb/^{204}Pb$ ratios displayed by some samples (Figs. 8 and 9). Despite significant variations within a given sub-province (Fig. 8, 9 and 11), all the Cretaceous magmatic provinces tend to show overlapping Sr-Nd-Pb isotopic compositions through time (Fig. 11). NES and TMR display $^{206}Pb/^{204}Pb$ and $^{208}Pb/^{204}Pb$ ratios similar to

those of the 14-0 Ma rocks from Madeira archipelago and Atlantis-Great Meteor Seamounts (Fig. 9). However, NES and most of the TMR lavas have $^{143}Nd/^{144}Nd$ lower than 0.5129 while the Madeira archipelago rocks have $^{143}Nd/^{144}Nd$ higher than 0.513. This could be explained by the trend shown by in the $^{143}Nd/^{144}Nd$ *vs.* $^{206}Pb/^{204}Pb$ plot, by the NES and in a lesser extent, the TMR lavas, toward the composition of the rocks from the ODP Site 1276 and Godzilla seamount which have distinct isotopic characteristics from the other Cretaceous rocks (Fig. 8b). Specifically, the ODP site 1276 sills and Godzilla Seamount lavas have lower $^{143}Nd/^{144}Nd$, $^{206}Pb/^{204}Pb$ and $^{208}Pb/^{204}Pb$ ratios (Figs. 8 and 9) that can be related to a stronger contribution of the EMI-like component. Indeed, Godzilla Seamount may represent one of the EMI type localities in the northern hemisphere (Geldmacher et al., 2008).

Plate reconstructions based on seafloor spreading anomalies show that, from the Cretaceous through to the present time, these alkaline magmatic occurrences are located between two concentric circles of ~1000 and 2500 km in diameter (Fig. 12). All northern Central Atlantic oceanic magmatism occurred on the periphery of a single ~25° × 20° area on the Earth's surface. This area is relatively fixed with respect to absolute plate motions, located at 5–32° West and 20–40° degrees north during the Cretaceous (Fig. 12). It should be noted that there is no magmatic activity outside this domain in the Central Atlantic throughout that entire period, with the exception of the Cape Verde Islands and the Bermuda Rise.

The above presented geochronological, geochemical, Sr–Nd–Pb isotopic data and plate reconstructions from the northern Central Atlantic and southern Northern Atlantic reveal that: (1) these alkaline magmatic provinces were active at the same time during the Cretaceous, (2) during this period of activity, these magmatic products were emplaced in the vicinity to each other on both sides of the mid Atlantic ridge, and (3) they share similar chemical characteristics in particular, isotopic ratios despite noticeable variations within each

province. These observations suggest that they should be considered as a part of a single magmatic province. The question remains by what mechanism this alkaline magmatism was triggered and, potentially, is still triggered today.

Models for the origin of Cretaceous Central Atlantic alkaline magmatism

Individual and random deep-seated Hawaii-type mantle plumes

All the alkaline Cretaceous magmatic provinces occurring in the northern Central Atlantic show similar chemical characteristics, in particular, overlapping isotopic compositions over a period of 110 Ma (Fig. 11). This is in contradiction to the significant variations of isotopic ratios through time observed on the Hawaii-Emperor seamounts chain (Regelous et al., 2003). This has never been observed for any Hawaiian-type mantle plume. Despite some variations within each province, this suggests the sampling by the magmatism of a common mantle source over a large area.

Based on the review of all the geological and geodynamical aspects of the Early Cretaceous alkaline magmatism in Northwest America (central New England and Quebec) and its possible connection with NES, the involvement of a Hawaii-type deep mantle plume has been challenged as an origin of the NES (McHone, 1996). In addition, the hypothesis suggesting that the Atlantis–Meteor Seamounts are the latest expression of the NES hot-spot track after the Corner Seamounts (Tucholke and Smoot, 1990) is not confirmed owing the lack of age from this seamount group. If we consider that the age of the magmatic activity on Atlantis-Meteor Seamounts is close to 17 Ma (Geldmacher et al., 2006), then there is a gap of approximately 60 Ma between the activity on the Corner and Atlantis–Meteor Seamounts. So far, there is no evidence of older magmatic activity on the Atlantis–Meteor Seamounts.

A single, flattened mantle plume head of 1000–2500 km in diameter (Campbell, 2007) is also not possible as magmatic products would be expected not only at the periphery of the ~1000–2500 km diameter region but also within its interior, which is not observed (Fig. 12). Chemical differences (different petrological rock types, variations in term of isotopic ratios) should be expected between the centre of the plume, where melting degree is higher and the deep mantle plume component is supposed to be mostly sampled and the rims of the plume head where melting degree is lower and the deep mantle source is more diluted with ambient mantle. Ultimately, a Hawaii-type or large-scale single mantle plume model is not a plausible explanation for the northern Central Atlantic and southern North Atlantic alkaline magmatic products.

Mantle plumes from a shared slab graveyard.

The stem of deep mantle plumes have an estimated average diameter of ~200 km (Campbell, 2007 and references therein). If each of the Cretaceous magmatic provinces (NES, TMR, Newfoundland Seamounts and Canary) originated from individually-rooted mantle plumes, this leads to a space issue of accommodating four mantle plumes in a relatively restricted area (1000 x 1000 km) at the time of their activity. To reconcile this unusual number of mantle plumes in a localized area, a large-scale deep process has to be considered. We posit that these deep mantle plumes may have formed at the periphery of a large slab graveyard located at either the ~660 km discontinuity or the core–mantle boundary, where deep mantle plumes allegedly originate (e.g. Morgan, 1971; Steinberger, 2000; Campbell, 2007). This slab graveyard would have been formed by the accumulation of oceanic lithospheres recycled into the mantle during ancient subductions, which might have begun during Pangea assembly around 500 Ma and eventually evolved to the circum-Pangea subduction just before 200 Ma. Several hundred million years would be required for large

slab sections to reach the ~660 km discontinuity, where their material would mature, mix with either ambient mantle and potentially rise toward the surface due to either their own buoyancy or dragged by deeper mantle plumes. This hypothesis is supported by the occurrence of numerous mantle plumes all over the Earth, starting during the Early Cretaceous period as expressed by the emplacement of several large igneous provinces (Kerguelen, Paraná-Etendeka, Ontong-Java; Coffin and Eldholm, 1994). Mantle plumes arising from the same slab graveyard would not only exhibit EMI and HIMU characteristics but share the same isotopic signatures.

The lack of alkaline magmatism within the ~1200–2500 km region (Fig. 12) is also explained by the fact that mantle plumes tend to form at the edges of slab graveyards, where the strongest convection takes place (Burke et al., 2008). In the center of slab graveyards, where the adjacent mantle struggles to convect, no plumes are produced. Hence, no magmatic products are found within the center of the ~1200–2500 km region in the northern Central Atlantic. As small-scale plumes originating from the slab graveyard, they can mix with the shallow Atlantic MORB mantle to form the observed chemical array between this mantle and subduction-related enriched components like EMI and HIMU.

Melting of a heterogeneous mantle source along lithospheric discontinuities.

McHone (1996) suggested that the magmatism of the NES could have been generated by the melting of a heterogeneous mantle along lithospheric discontinuities. Edge-driven convection (e.g. Anderson, 1994; King and Ritsema, 2000) at continental–oceanic lithospheric interfaces could also facilitate partial melting and upward ascent of magma via lithospheric discontinuities. This process could explain the convoluted and multiple chains of seamounts (e.g., NES, Newfoundland Seamounts, Fogo Seamounts). Such a hypothesis has been suggested to explain the distribution of magmatism on TMR (Geldmacher et al., 2008, Merle et al., 2006, 2018). However, this hypothesis presents several issues: (1) there are

many areas in the Atlantic Ocean proximal to lithospheric discontinuities that are not associated with magmatic activity (Matton and Jebrak, 2009), (2) decompression melting along an oceanic fracture zone would likely involve melting the asthenosphere then produce MORB-like melts yet none of the volcanic provinces considered here show a MORB affinity, and (3) in the case of volcanic provinces straddling the ocean–continent boundary (e.g., the Cameroon Volcanic Line), there is no major chemical difference between the volcanic rocks emplaced over continental or oceanic sectors, both of which display OIB-like signatures (e.g. Merle et al., 2017). Therefore, decompression melting along lithospheric discontinuities cannot fully explain the nature and distribution of alkaline magmatic products in the northern Central Atlantic and the presence of an enriched component in the vicinity of the lithospheric discontinuities is required to explain the chemistry of the rocks.

Melting of shallow mantle chemical anomaly.

An alternative model to explain the origin of this widespread magmatism is to consider a large, relatively shallow melting anomaly emitting pulses of magmas (Merle et al., 2009). Such shallow source would explain the range of Dy/Yb ratio (1.5-2.2) observed in the NES sample that suggests a small amount of residual garnet in the source. A similar hypothesis has been suggested to explain the coeval (s.l.) magmatism and rather similar isotopic characteristics of the Madeira and Canary archipelagos (Mata et al., 1998). This magmatism would have originated from a low-velocity mantle anomaly extending over a 2500 km × 4000 km area and ~100-200 km deep presently residing under Western Europe and the eastern Atlantic Ocean (Hoernle et al., 1995). This sub-lithospheric low-velocity mantle, could be the source of the Cenozoic circum-Mediterranean anorogenic magmatism (Hoernle et al., 1995; Lustrino and Wilson, 2007). However, it is uncertain whether this low-velocity mantle anomaly was already present during the Cretaceous.

Although some isotopic characteristics of the Cretaceous rocks are close to HIMU (Figs. 8 and 9), some Cretaceous TMR and NES samples plot below the NHRL in the Pb isotopic plots (Fig. 9). Such a feature has been interpreted as the involvement in the source of a younger oceanic crust (~1400-400 Ma, Thirlwall, 1997). Specifically, the HIMU-like Pb isotopic signatures of the Madeira archipelago are compatible with the involvement of a ~900 Ma recycled oceanic lithosphere present in a deep mantle plume (Geldmacher and Hoernle, 2000, 2001). Therefore, we suggest that such a young HIMU-like component is present in the source of the NES samples. Alternatively, this HIMU component could originate from supra-subduction mantle remnants preserved in the Atlantic oceanic lithosphere at ODP Site 1277 (located in the immediate vicinity of ODP Site 1276; Fig. 1) and underneath the Lion and Dragon Seamounts on the southern TMR (Müntener and Manatschal, 2006; Merle et al., 2012). If valid, this hypothesis would definitively confirm the melting of a shallow source instead of a deep mantle plume as the origin of the alkaline magmatism in this region.

Also observed is a trend with decreasing $^{143}Nd/^{144}Nd$ and $^{206}Pb/^{204}Pb$ ratio toward an EMI component (Fig. 8b), defined essentially by some SW Portugal and NES samples, the ODP Site 1276 sills and the rocks from Godzilla Seamount (Figs. 8b and 9). However, this trend shows no temporal control on the chemical characteristics of the mantle source. Indeed, rocks from Godzilla Seamount have the same age as those from SW Portugal but show a much stronger EMI affinity (Fig. 11). The ODP Site 1276 sills and Godzilla seamount rocks are distinct from the other rocks by having lower $^{143}Nd/^{144}Nd$, $^{206}Pb/^{204}Pb$ and $^{208}Pb/^{204}Pb$ ratios compared to the other samples, which are rather similar to those of Atlantis Seamount and Madeira archipelago (Figs. 8, 9 and 11). As there is no clear space–time progression for the occurrence of this EMI component in the lavas of the Cretaceous magmatic province in northern Central Atlantic and southern North Atlantic, this suggests that the source of these magmas is rather a large-scale heterogeneous mantle. This hypothesis is supported by the

North Oceanographer fracture Zone MORB (Dosso et al., 1999), which still samples this source component. Furthermore, despite some variations within each of the sub-provinces, the isotopic ratios overlap the compositions of those found in the recent Madeira archipelago and Atlantis–Meteor Seamounts. As a consequence, we suggest that the Cretaceous magmatism of the TMR, NES, ODP Site 1276 sills could have been produced by a large mantle melting anomaly containing small-scale EMI-like heterogeneities. Melting of such a mantle source probably lasted until the present-day to produce Cenozoic magmatism on TMR, the Madeira archipelago, and the Atlantis–Meteor Seamounts.

The nature of the EMI end-member remains debated (e.g. Zindler and Hart, 1986, Lustrino and Dallai, 2003; Collerson et al., 2010). It has been interpreted as: (1) recycling into the deep mantle by subduction of various material, including lower continental crust, subcontinental lithospheric mantle, oceanic lithosphere (crust and/or mantle) potentially metasomatised with old pelagic or terrigenous sediments and eventually carried back to the surface by mantle plumes (White, 1985; Tatsumoto and Nakamura, 1991; Weaver, 1991, Chauvel et al., 1992; Woodhead et al., 1993; Rehkämper et al., 1997; Eisele et al., 2002; Niu and O'Hara, 2003); (2) delamination of sub-continental lithospheric mantle in the shallow mantle (Hoernle et al., 2011), and (3) a metasomatised mantle wedge recycled into the shallow mantle (Kempton et al., 2002). According to this latter definition, the preserved sections of supra-subduction zone mantle found at ODP Site 1277 and on the Lion and Dragon Seamounts (Müntener and Manatschal, 2006; Merle et al., 2012) could be the origin of the EMI chemical anomaly. This hypothesis leads to question the nature of the material carrying the HIMU signature. A possibility is that pelagic sediments associated with the oceanic lithosphere, which eventually formed the sub-arc mantle remnants, could have been also incorporated into the Atlantic oceanic lithosphere or are present in the topmost

asthenosphere. However, there are no isotopic data for the mantle remnants from ODP Site 1277 and TMR and therefore this hypothesis has not been confirmed so far.

Conclusions

Our new ages combined with the filtered dataset from the dated NES samples reveal that there is no robust age trend along the NES. The ages and Sr–Nd–Pb isotopic signatures of the NES magmatism share similarities with those of the TMR, ODP Site 1276 sills, SW Portugal and, potentially, the Corner and Newfoundland Seamounts. All these magmatic provinces were active between 105 and 70 Ma. This magmatic activity might have been coeval to the CISP, which was active since at least 126 Ma and potentially as early as 142 Ma but this has to be confirmed by reliable data. CISP and TMR also lasted until the last million years.

Our new age and isotopic data for the JAR samples indicates that the JAR originated from on the activity of the Mid-Atlantic ridge around 120 Ma. The coeval magmatic activity and overlapping range of isotope ratios shown by these Cretaceous magmatic provinces justify considering them as a single magmatic province. The presence of a small-scale EMI-like component in the chemical characteristics of some of the TMR, NES and ODP Site 1276 rocks argue for the melting of a heterogeneous mantle. This EMI component seems to be sampled randomly in term of location and through time that cannot be explained by chemically-distinct, Hawaii-type plumes. The presence in the Atlantic oceanic lithosphere or shallow asthenosphere of supra-subduction zone mantle remnants could account for this EMI-type chemical heterogeneity.

ACKNOWLEDGEMENTS

We thank the International Ocean Discovery Program (IODP), in particular the IODP core library in Bremen which provided the samples from DSDP leg 43, and the Australia-New Zealand IODP Consortium (ANZIC), which provided Legacy/Special Analytical Funding for this study. ANZIC is supported by the Australian Government through the Australian Research Council's LIEF funding scheme [LE0882854] and the Australian and New Zealand consortium of universities and government agencies. C. Mayers and R.A. Frew of the WA Argon lab are also thanked for providing technical assistance for sample preparation and analysis.

References

Anderson, D.L., 1994. The sublithospheric mantle as the source of subcontinental flood basalts; the case against the continental lithosphere and plume head reservoir. Earth Planet. Sci. Lett. 123, 269-280.

Baksi, A.K., 2007. A quantitative tool for detecting alteration in undisturbed rocks and minerals—I: Water, chemical weathering, and atmospheric argon. Geol. Soci. Am. Spec. Pap. 430, 285-303.

Burke, K., Steinberger, B., Torsvik, T.H., Smethurst, M.A., 2008. Plume Generation Zones at the margins of Large Low Shear Velocity Provinces on the core–mantle boundary, Earth Planet. Sci. Lett. 265, 49-60.

Chauvel, C., Hofmann, A.W., Vidal, P., 1992. HIMU-EM: the French Polynesian connection. Earth Planet. Sci. Lett. 110, 99-119.

Coffin, M.F., Eldholm, O., 1994. Large igneous provinces: Crustal structure, dimensions, and external consequences. Rev. Geophys. 32, 1-36.

Collerson, K.D., Williams, Q., Ewart, A.E., Murphy, D.T. 2010. Origin of HIMU and EM-1 domains sampled by ocean island basalts, kimberlites and carbonatites: The role of CO2-fluxed lower mantle melting in thermochemical upwellings. Phys. . Earth . Planet. Int. 181, 112-131.

Campbell, I.H., 2007. Testing the plume theory, Chem. Geol. 241, 153-17.

Cann, J.R., 1979. Metamorphism of oceanic crust. In: Talwani, M., Hayes, D.E. (eds.) Deep drilling results in the Atlantic ocean: ocean crust. America Geophysical Union Geodynamic Service, 230-238.

Caroff, M., Bellon, H., Chauris, L., Carron, J.-P., Chevrier, S., Gardinier, A., Cotten, J., Le Moan, Y. Neidhart, Y., 1995. Magmatisme fissural triasico-liasique dans l'ouest du Massif Armoricain (France): pétrologie, géochimie, âge, et modalités de la mise en place. Can. J. . Earth Sci. 32, 1921-1936.

Dalrymple, G.B., Clague, D.A., 1976. Age of the Hawaiian-Emperor bend. Earth and Planetary Sciences Letters 31, 313-329.

D'Oriano, F., Angeletti, L., Capotondi, L., Laurenzi, M. A., López Correa, M., Taviani, M., Torelli, L., Trua, T., Vigliotti, L., Zitellin, N. 2010. Coral Patch and Ormonde seamounts as a product of the Madeira hot-spot, Eastern Atlantic Ocean. Terra Nova*, 22*, 494–500.

Dosso, L., Bougault, H., Langmuir, C., Bollinger, C., Bonnier, O., Etoubleau, J., 1999. The age and distribution of mantle heterogeneity along the Mid-Atlantic Ridge (31–41°N). Earth Planet. Sci. Lett. 170, 269-286.

Doubrovine, P.V., Steinberger, B., Torsvik, T.H., 2012, Absolute plate motions in a reference frame defined by moving hot spots in the Pacific, Atlantic, and Indian oceans. J. Geophys. Res. 117, B09101.

Duncan, R.A., 1984. Age progressive volcanism in the New England Seamounts and the opening of the central Atlantic Ocean. J. . Geophys. Res. 89, 9980-9990.

Eisele, J., Sharma, M., Galer, S.J.G., Blichert-Toft, J., Devey, C.W., Hofmann, A.W., 2002. The role of sediment recycling in EM-I inferred from Os, Pb, Hf, Nd, Sr isotope and trace element systematics of the Pitcairn hot-spot. Earth Planet. Sci. Lett. 196, 197-212.

Foland, K.A., Faul H., 1977. Age of the White Mountain intrusives-New Hampshire, Vermont and Maine, USA, Am. J. Sci. 277, 888-904.

Foland, K.A., Gilbert, L.A., Sebring, C.A., Jiang-Feng, C., 1986. $^{40}Ar/^{39}Ar$ ages for plutons of the Monteregian Hills, Quebec: Evidence for a single episode of Cretaceous magmatism. Geol. Soc. Am. Bull. 97, 966-974.

Geldmacher, J., Hoernle, K., The 72 Ma geochemical evolution of the Madeira hot-spot (eastern North Atlantic): recycling of Paleozoic (≤ 500 Ma) oceanic lithosphere, Earth Planet. Sci. Lett. 183, 73-92, 2000.

Geldmacher, J., Hoernle, K., Corrigendum to 'The 72 Ma geochemical evolution of the Madeira hot-spot (eastern North Atlantic): recycling of Paleozoic (≤ 500 Ma) oceanic lithosphere', Earth Planetary Sci. Lett. 186, 333, 2001.

Geldmacher, J., Van den Bogaard, P., Hoernle, K., Schmincke, H.U., 2000. The $^{40}Ar/^{39}Ar$ age dating of the Madeira Archipelago and hot-spot track (eastern North Atlantic). Geoch. Geophys. Geosyst. 1, doi: 10.1029/1999GC000018.

Geldmacher, J., Hoernle, K., Van den Bogaard, P., Duggen, S., Werner, R., 2005. New $^{40}Ar/^{39}Ar$ age geochemical seamounts Canary and Madeira volcanic provinces: Support for the mantle plume hypothesis. Earth Planet. Sci. Lett. 237, 85-101.

Geldmacher, J., Hoernle, K., Klügel, A., Van den Bogaard, P., Wombacher, F., Berning, B., 2006. Origin and geochemical evolution of the Tore-Madeira Rise (eastern North Atlantic). J. Geophys. Res., B09206. doi:10.1029/2005JB003931.

Geldmacher, J., Hoernle, K., Klügel, A., Van der Bogaard, P., Bindeman, I., 2008. Geochemistry of a new enriched mantle type locality in the northern hemisphere: Implications for the origin of the EM-I source. Earth Planet. Sci. Lett. 265, 167-182.

Gente, P., Dyment, J., Maia, M., Goslin, J. 2003. Interaction between the Mid-Atlantic Ridge and the Azores hot-spot during the last 85 Myr: emplacement and rifting of the hot-spot-derived plateaus. Geochem. Geophys. Geosyst. 4, doi:10.1029/2003GC0052.

Gradstein, F.M., Ogg, J.G. & Smith, A.G. (eds), 2004. A geological time scale. Cambridge Univ. Press, Cambridge, 500 pp.

Grange, M., Schärer, U., Merle, R., Girardeau, J., Cornen, G., 2010. Plume-Lithosphere interaction during migration of Cretaceous Alkaline Magmatism in SW Portugal: Evidence from U-Pb Ages and Pb-Sr-Hf Isotopes. J. Petrol. 51, 1143-1170.

Griffiths, R.W., Campbell, I.H., 1990. Stirring and structure in mantle starting plumes. Earth Planet. Sci. Lett. 99, 66-78.

Hart, S.R., 1984. A large scale isotopic anomaly in the southern hemispheric mantle. Nature 309, 753-757.

Hart, S.R., Blusztajn, J., 2006. Age and geochemistry of the mafic sills, ODP site 1276, Newfoundland margin. Chem. Geol. 235, 222-237.

Heaman, L.M., Kjarsgaard, B.A., 2000. Timing of eastern North American kimberlite magmatism: continental extension of the Great Meteor hot-spot track? Earth Planet. Sci. Lett. 178, 253-268.

Hoernle, K., Zhang, Y.S., Graham, D., 1995. Seismic and geochemical evidence for large-scale mantle upwelling beneath the eastern Atlantic and western and central Europe. Nature 374, 34-39.

Hoernle, K., Hauff, F., Werner, R., van den Bogaard, P., Gibbons, A.D., Conrad, S. and Muller, R.D., 2011. Origin of Indian Ocean Seamount Province by shallow recycling of continental lithosphere. Nature Geosci. 4, 883-887.

Hofmann, C., Féraud, G. Courtillot, V., 2000. $^{40}Ar/^{39}Ar$ dating of mineral separates and whole rocks from the Western Ghats lava pile: further constraints on duration and age of the Deccan traps. Earth Planet. Sci. Lett. 180, 13-27.

Honnorez, J. 1981. The aging of the oceanic crust at low temperature. In: Emiliani, C. (eds.) The sea: the oceanic lithosphere, Wiley, New York, 525-587.

Houghton, R.L., 1979. Petrology and geochemistry of basaltic rocks recovered on Leg 43 of the Deep Sea Drilling Project. Init. Rep. Deep Sea Drilling Proj. 43, 721-738.

Houghton, R.L., Thomas, J.E. Jr., Diecchio R.J., Tagliacozzo A., 1979. Radiometric ages of basalts from DSDP Leg 43: Sites 382 and 385 (New England Seamounts), 384 (J-anomaly), 386 and 387 (central and western Bermuda Rise), Init. Rep. Deep Sea Drilling Proj. 43, 739-754.

Kempton, P.D., Pearce, J.A., Barry, T.L., Fitton, J.G., Langmuir, C., Christie, D.M., 2002. Sr-Nd-Pb-Hf isotope results from ODP Leg 187: evidence for mantle dynamics of the Australian–Antarctic discordance and origin of the Indian MORB Source. Geochem. Geophys. Geosyst. 3, 1074.

King, S.D., Ritsema, J., 2000. African Hot Spot Volcanism: Small-Scale Convection in the Upper Mantle Beneath Cratons. Science 290, 1137-1139.

Klugel, A., Hansteen, T.H., van den Bogaard, P., Strauss, H., Hauff, F., 2011. Holocene fluid venting at an extinct Cretaceous seamount, Canary archipelago. Geology 39, 855-858.

Louden, K.E., Tucholke, B.E., Oakey, G.N., 2004. Regional anomalies of sediment thickness, basement depth and isostatic crustal thickness in the North Atlantic Ocean, Earth Planet. Sci. Lett. 224, 193-211.

Lustrino, M., Wilson M., 2007. The circum-Mediterranean anorogenic Cenozoic igneous province. Earth Sci. Rev. 81, 1-65.

Lustrino, M., Dallai, L., 2003. On the origin of the EM-I end-member. N. J. Min. Abh. 179, 85-100.

Mata, J., Kerrich, R., MacRae, N.D., Wu, T.-W., 1998. Elemental and isotopic (Sr,Nd, and Pb) characteristics of Madeira Island basalts: Evidence for a composite HIMU–EM I plume fertilizing lithosphere. Can. J. Earth Sci. 35, 980-997.

Matton, G., Jebrak, M., 2002. The Cretaceous Peri-Atlantic Alkaline Pulse (PAAP): Deep mantle plume origin or shallow lithospheric break-up? Tectonophys. 469, 1-12.

McHone, J.G., 1996. Constraints on the mantle plume model for Mesozoic alkaline intrusions in northeastern North America. Can. Min. 34, 325-334.

Merle, R., Scharer, U., Girardeau, J. Cornen, G., 2006. Cretaceous seamounts along the ocean-continent of Iberian margin: U-Pb ages and Sr-Pb-Hf isotopes. Geochim. Cosmochim. Acta 70, 4950-4976.

Merle, R., Jourdan, F., Marzoli, A., Renne, P.R., Grange, M., Girardeau, J., 2009. Evidence of multi-phase Cretaceous to Quaternary alkaline magmatism on Tore–Madeira Rise and neighbouring seamounts from $^{40}Ar/^{39}Ar$ ages. J. Geol. Soc. London 166, 879-894.

Merle, R., Kaczmarec, M.-A., Tronche, E., Girardeau, J., 2012. Occurrence of inherited supra-subduction zone mantle in the oceanic lithosphere as inferred from mantle xenoliths and xenocrystals from Dragon and Lion seamounts (Southern Tore-Madeira Rise). J. Geol. Soc. London 169, 251-267.

Merle, R., Marzoli, A., Aka, F.T., Chiaradia, M., Reisberg, L., Castorina, F., Jourdan, F., Renne, P.R., N'ni, J., Nyobe, J.B., 2017. Mt Bambouto Volcano, Cameroon Line: Mantle Source and Differentiation of Within-plate Alkaline Rocks. J. Petrol. 58, 933-962.

Merle, R., Jourdan, F., Girardeau, J., 2018. Geochronology of the Tore-Madeira Rise seamounts and surrounding areas: a review. Aus. J. Earth Sci. 65, 591-605.

Meschede, M., A method of discriminating between different types of mid-ocean ridge basalts and continental tholeiites with the Nb-Zr-Y diagram, Chem. Geol. 56, 207-218, 1986.

Miranda, R., Valadares, V., Terrinha, P., Mata, J., Do Rosario Azevedo, M., Gaspara, M., Kullberg, J.C., Ribeiro, C., 2009. Age constraints on the Late Cretaceous alkaline magmatism on the West Iberian Margin. Cret. Res. 30, 575-586.

Morgan, W.J., 1971. Convection plumes in the lower mantle. Nature 230, 42-43.

Morgan, W.J., 1983. Hot-spot tracks and the early rifting of the Atlantic. Tectonophys. 94, 123-139.

Müntener, O., Manatschal, G., 2006. High degrees of melting recorded by spinel harzburgites of the Newfoundland margin: The role of inheritance and consequences for the evolution of the southern North Atlantic. Earth Planet. Sci. Lett. 252, 437-452.

Nirrengarten M., Manatschal G., Tugend J., Kusznir N.J., Sauter D., 2017. Nature and origin of the J-magnetic anomaly offshore Iberia–Newfoundland: implications for plate reconstructions. Terra Nova 29, 20-28.

Nirrengarten, M., Manatschal, G., Tugend, J., Kusznir, N., Sauter, D., 2018. Kinematic evolution of the southern North Atlantic: Implications for the formation of hyperextended rift systems. Tectonics 37, 89-118.

Niu, Y., O'Hara, M.J., 2003.Origin of ocean island basalts: a new perspective from petrology, geochemistry, and mineral physics considerations, J. Geophys. Res. 108, 2209.

O'Neill, C., Müller, D., Steinberger, B., 2005. On the uncertainties in hot spot reconstructions and the significance of moving hot spot reference frames. Geochem. Geophys. Geosyst. 6, Q04003, DOI 10:1029/2004GC000784.

Pearce, J.A., Norry, M.J., 1979. Petrogenetic implications of Ti, Zr, Y, and Nb variations involcanic rocks. Contrib. Min. Petrol. 69, 33–47.

Pearce, J.A., 1982. Trace element characteristics of lavas from destructive plate boundaries. In: Thorpe, R.S. (Eds.), Andesites. John Wiley and Sons., New York, pp. 525-548.

Pearce, J.A., 2008. Geochemical fingerprinting of oceanic basalts with applications to ophiolite classification and the search for Archean oceanic crust. Lithos 100, 14-48.

Regelous, M., Hofmann, A.W., Abouchami, W., Galer, S.J.G., 2003. Geochemistry of Lavas from the Emperor Seamounts, and the Geochemical Evolution of Hawaiian Magmatism from 85 to 42 Ma, J. Petrol. 44, 113–140.

Rehkämper, M., Hofmann, A.W., 1997. Recycled ocean crust and sediment in Indian Ocean MORB. Earth Planet. Sci. Lett. 147, 93-106.

Renne, P., Sprain, C.J., Richards, M.A., Self, S., Vanderkluysen, L., Pande, K., 2015. State shift in Deccan volcanism at the Cretaceous-Paleogene boundary, possibly induced by impact. Science, 350, 76-78.

Ribeiro Pinto, L., Martins, S., Hildenbrand, A., Madureira, P., Mata, J., 2017. The genetic link between the Azores Archipelago and the Southern Azores Seamount Chain (SASC): The elemental, isotopic and chronological evidences. Lithos 294–295, 133-146.

Ryan, W.B.F., Carbotte, S.M., Coplan, J.O., O'Hara, S., Melkonian, A., Arko, R., Weissel, R.A., Ferrini, V., Goodwillie, A., Nitsche, F., Bonczkowski, J., Zemsky, R., 2009. Global Multi-Resolution Topography synthesis. Geochem. Geophys. Geosyst. 10, Q03014, DOI:10.1029/2008GC002332.

Seton, M., Müller, R. D., Zahirovic, S., Gaina, C., Torsvik, T., Shephard, G., Talsma, A., Gurnis, M., Turner, M., Maus, S., Chandler, M., 2012. Global continental and ocean basin reconstructions since 200 Ma. Earth-Sci. Rev. 113, 212-270.

Steinberger, B., 2000. Plumes in a convecting mantle: Models and observations for individual hot-spots. J. Geophys. Res. 105, 11127-11152.

Steinberger, B., Sutherland, R., O'Connell, R.J., 2004. Prediction of Emperor-Hawaii seamount locations from a revised model of global plate motion and mantle flow. Nature 430, 167-173.

Sleep, N.H., 1990. Monteregian hot-spot track: A long-lived mantle plume. J. Geophys. Res. 95, 21983-21990.

Sullivan, K.D., Keen C.E., 1977. Newfoundland seamounts: Petrology andgeochemistry, Geol. Assoc. Canada Spec. Paper 16, 461-476.

Sun, S.S., McDonough, W.F., 1989. Chemical and isotopic systematics of oceanic basalts: implication for mantle composition and processes, in: Saunders, A.D., Norry, M.J. (eds.), Magmatism in the ocean basins, Geol. Soc. Spec. Publ. 42, 313-345.

Taras, B.D., Hart, S.R., 1987. Geochemical evolution of the New England seamount chain: isotopic and trace element constraints. Chem. Geol. 64, 35-54.

Tatsumoto, M., and Y. Nakamura, DUPAL anomaly in the sea of Japan: Pb, Nd, and Sr isotopic variations at the eastern Eurasian continental margin, Geochim. Cosmoch. Acta, 55, 3697-3708, 1991.

Thirlwall, M.F., 1997. Pb isotopic and elemental evidence for OIB derivation from young HIMU mantle. Chem. Geol. 139**,** 51–74.

Tucholke, B.E., and the shipboard scientific party, 1979. Site 384. The Cretaceous/Tertiary boundary, Aptian reefs, and the J-Anomaly Ridge, Init. Rep. Deep Sea Drilling Proj. 43, 107-165.

Tucholke, B.E., Ludwig, W.J., 1982. Structure and origin of the J Anomaly Ridge, Western North Atlantic Ocean. J. Geophys. Res. 87, 9389-9407.

Tucholke, B.E., Smoot, N.C., 1990. Evidence for age and evolution of Corner Seamounts and Great Meteor Seamount Chain from multibeam bathymetry. Journal of Geophysical Research 95, 17555-17569.

Tucholke, B.E., Vogt, P.R. 1979. Introduction and explanatory notes, Leg 43 Deep Sea Drilling Project, (western North Atlantic). Init. Rep. . Deep Sea Drilling Proj. 43, 5-28.

Van den Bogaard, P., 2013. The origin of the Canary Island Seamount Province - New ages of old seamounts. Sci. Reports, 3.

Verati, C., Jourdan, F., 2014, Modelling effect of sericitization of plagioclase on the $^{40}K/^{40}Ar$ and $^{40}K/^{39}Ar$ chronometers: Implication for dating basaltic rocks and mineral deposits: Geol. Soc. Special Publ. 378, 155-174.

Weaver, B.L., 1991. The origin of ocean island basalt end-member compositions: trace element and isotopic constraints. Earth Planet. Sci. Lett. 104, 381-397.

Wendt, I., Kreuzer, H., Muller, P., Von Rad, U., Raschka, H., 1976. K-Ar age of basalts from Great Meteor and Josephine seamount (eastern North Atlantic). Deep-Sea Res. 23, 849-862.

Wilson, J.T., 1963. A possible origin of the Hawaiian Islands. Can. J. Phys. 41, 863-870.

White, W.M., 1985. Sources of oceanic basalts: radiogenic isotopic evidence. Geology 13, 115-118.

Whittaker, J.M., Afonso, J.C., Masterton, S., Mueller, R.D., Wessel, P., Williams, S.E., Seton, M., 2015. Long-term interaction between mid-ocean ridges and mantle plumes. Nature Geosci. 8, 479-484.

Woodhead, J.D., Greenwood, P., Harmon, R.S., Stoffers, P., 1993. Oxygen isotope evidence for recycled crust in the source of EM type ocean island basalts. Nature 362, 809-813.

Zindler, A., Hart, S.R., 1986.Chemical geodynamics. Annual Review Earth Planet. Sci. 14, 493-571.

Figure captions

Fig. 1: Topographic and bathymetric map of the Central Atlantic Ocean and surrounding continents with major alkaline seamounts and ocean island provinces labelled. Map made using GeoMapApp (Ryan et al., 2009). FZ: Fracture Zone. See text for references of seamount ages.

Fig. 2: Bathymetric map of the New England Seamount Chain and J-anomaly Ridge, annotated with new ages and published age estimates (Houghton et al., 1978; Duncan, 1984). Map made using GeoMapApp (Ryan et al., 2009). Smt.: Seamount.

Fig. 3: Photographs of hand specimen of rocks from New England seamounts (a-d) and J-anomaly ridge (e). (a): Breccia with basaltic clast from Nashville seamount. (b): Very vesicular basaltic fragment from Vogel seamount. (c): Slab of basalt from Vogel seamount showing phenocrystals of olivine completely oxidised and pyroxene. Note the vacuoles filled with calcite. (d): Slightly vesicular fragment of basalt from Vogel seamount. (e): green-coloured fragments from J-anomaly ridge. Note the large vacuoles filled with green and white alteration material.

Fig. 4: Microphotographs of thin sections of the NES and JAR samples. (a): Large amphibole phenocrystal from Nashville seamount (NES2). (b): clinopyroxene phenocrystal from Vogel seamount (NES10). (c): Low-temperature seawater alteration shown by crystallisation of fibrous zeolite in vesicle. Example from Nashville seamount. (d) Aphyric sample from Vogel seamount (NES7) with microlithic groundmass (plagioclase+Fe-Ti oxide). (e): Porphyritic sample from JAR. Seawater alteration is evidenced by crystallisation of calcite in the

vesicles. (f) Detail of an altered olivine phenocrystal partly transformed into bowlingite (green alteration phase) and oxidised.

Fig. 5: $^{40}Ar/^{39}Ar$ apparent age and related K/Ca ratio spectra of the hornblende and groundmass separates versus the cumulative percentage of ^{39}Ar released for samples from New England Seamounts (NES) and J-anomaly Ridge (JAR). Errors on plateau and mini-plateau ages are quoted at 2σ and do not include systematic errors (i.e. uncertainties on the age of the monitor and on the decay constant). MSWD and probability are indicated. See online supplementary material for full $^{40}Ar/^{39}Ar$ data tables.

Fig. 6: Geotectonic discriminant diagrams. (a) Triangular plot Nb-Zr-Y (Meschede, 1986); (b) Ta/Yb *vs* Th/Yb plot (Pearce, 1982); (c) Zr *vs* Zr/Y plot (Pearce and Norry, 1979).

Fig. 7**:** Rare earth elements and incompatible trace element patterns of new and published NES in (a) and (c) and JAR samples in (b) and (d). Normalisation and N-MORB, E-MORB and OIB patterns after Sun and McDonough (1989).Previously published data from Houghton (1979) for the JAR samples and from Houghton et al.(1979) and Taras and Hart (1987) for the NES samples.

Fig. 8: (a) $^{143}Nd/^{144}Nd$ *vs*. $^{87}Sr/^{86}Sr$ and (b) $^{143}Nd/^{144}Nd$ *vs*. $^{206}Pb/^{204}Pb$ plots showing the initial ratios of NES. Note that the $^{206}Pb/^{204}Pb$ ratios for JAR samples are measured and not back-calculated to initial (see details in text). Also shown the NES data from literature (Taras and Hart, 1987) as well as data from TMR and surrounding seamounts (Bernard-Griffith et al., 1997; Geldmacher et al., 2005, 2006, 2008), SW Portugal (Bernard-Griffith et al., 1997)

and ODP site 1276 sills (Hart and Blusztajn, 2006). Isotopic fields for Atlantic MORB, Madeira and Canary Islands from GEOROC database.

Fig. 9: $^{207}Pb/^{204}Pb$ *vs.* $^{206}Pb/^{204}Pb$ and $^{208}Pb/^{204}Pb$ *vs.* $^{206}Pb/^{204}Pb$ plots showing the new initial isotopic ratios of NES and other northern Central Atlantic alkaline magmatic provinces. Note that JAR data has not been back-calculated to initial. Same data references as in Fig. 8. Anomalous value of $^{207}Pb/^{204}Pb$ ratio from NES 7 (Vogel seamount) is not plotted (see text for further details).

Fig. 10: Age *vs.* latitude for the NES samples from this study and literature (Houghton et al., 1978, Duncan, 1984). (a) Unfiltered dataset. The data shown in light grey were obtained by K-Ar and $^{40}Ar/^{39}Ar$ single-step total fusion techniques and are considered unreliable. (b) Filtered dataset. The errors bars represent 2σ errors and are smaller than the symbols for the step-heated $^{40}Ar/^{39}Ar$ data.

Fig. 11: Age vs initial isotopic ratios for NES, TMR, SW Portugal and ODP site 1276 sills. . Same data references as for Fig. 5. The grey band represents the range of overlapping compositions.

Fig. 12: Plate reconstructions of the Central Atlantic made using GPlates software, version 1.5, using the rotation poles, plate polygons, magnetic lineations and mid-ocean ridges of Seton et al. (2012). Fracture zones were manually added using known present-day fracture zones patterns as those in Seton et al. (2012) were incomplete. The positions of fixed mantle

plumes from Whittaker et al. (2015) were used as present-day positions but were modified back in time to include a moving hot-spot reference frame developed by Doubrovine et al. (2012).

Highlights

- We made $^{40}Ar/^{39}Ar$ dates for New England Seamounts (NES) and J-anomaly ridge (JAR).
- We present the first Sr-Nd-Pb isotopic ratios for JAR and new Sr-Nd-Pb data for NES.
- The NES magmatic activity occurred at 100-82 Ma.
- JAR yielded an alteration age of 76 Ma but likely formed around 120 Ma.
- Source of the Cretaceous magmatism in Central Atlantic is an heterogenous mantle.

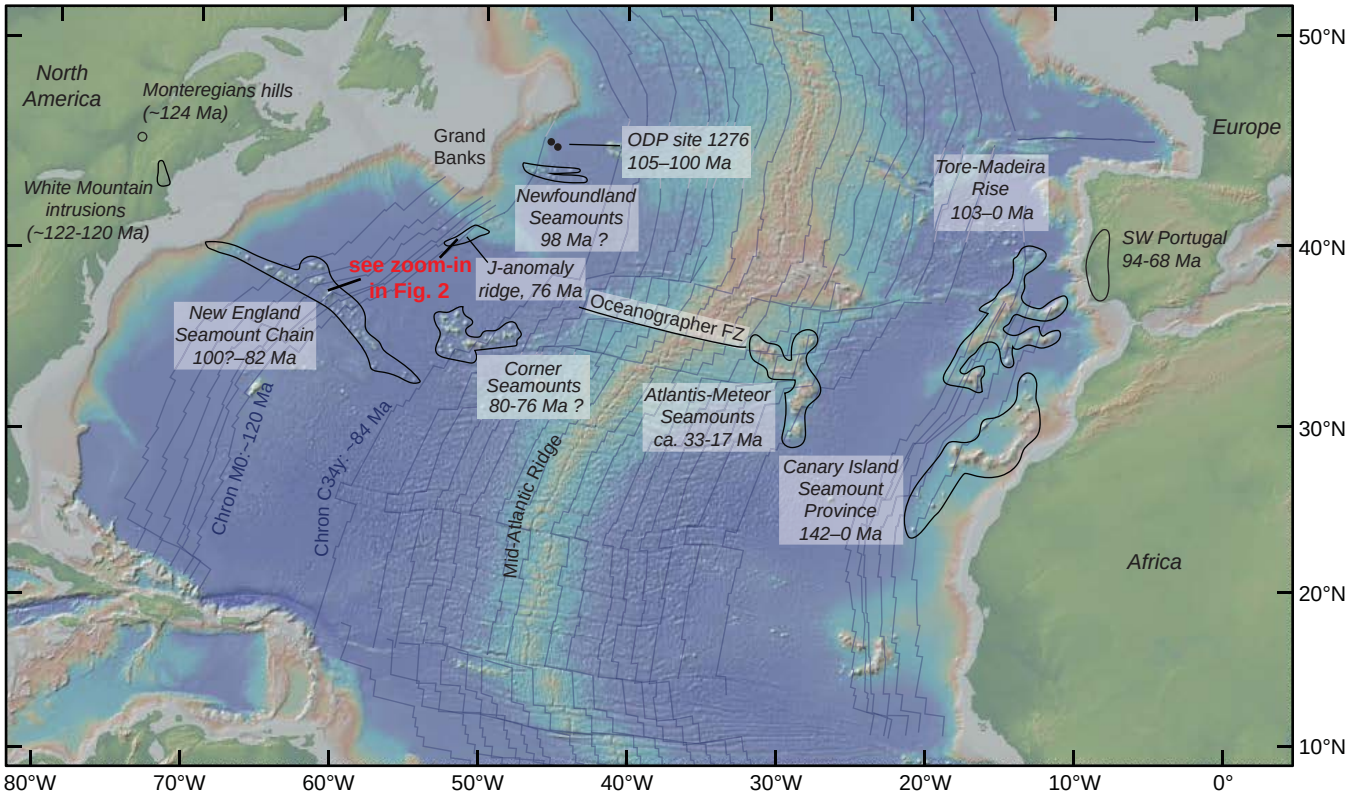

Merle et al., Figure 1

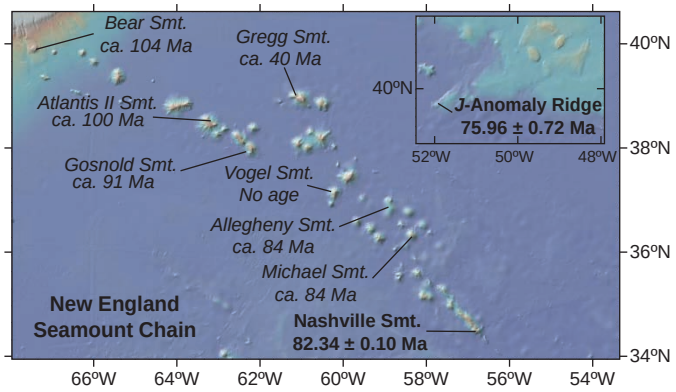

Merle et al., Figure 2

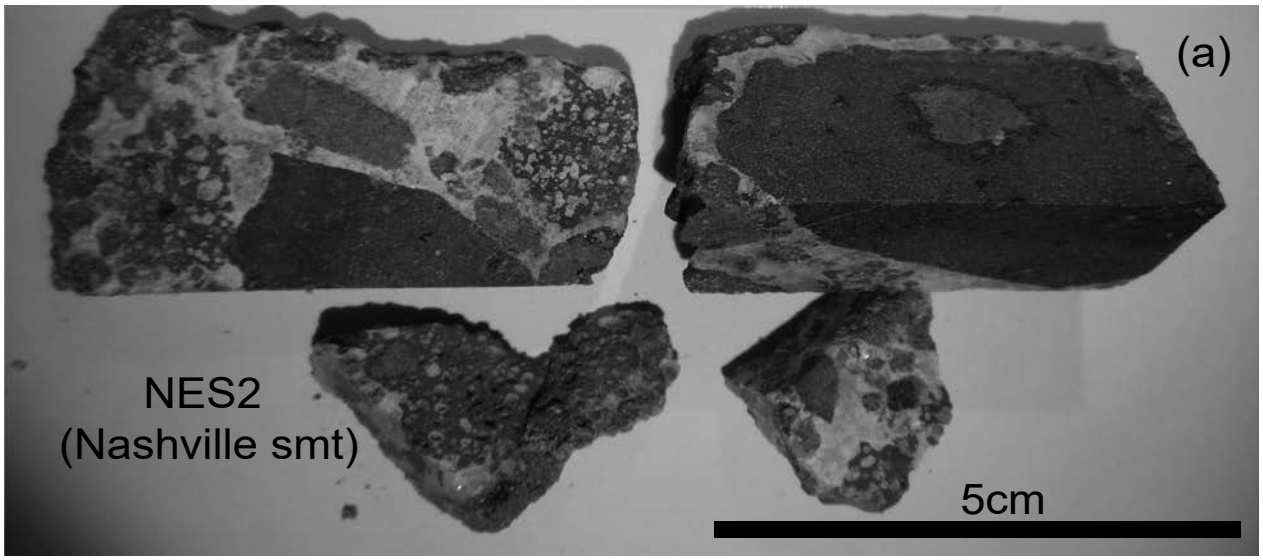
(a)
NES2
(Nashville smt)
5cm

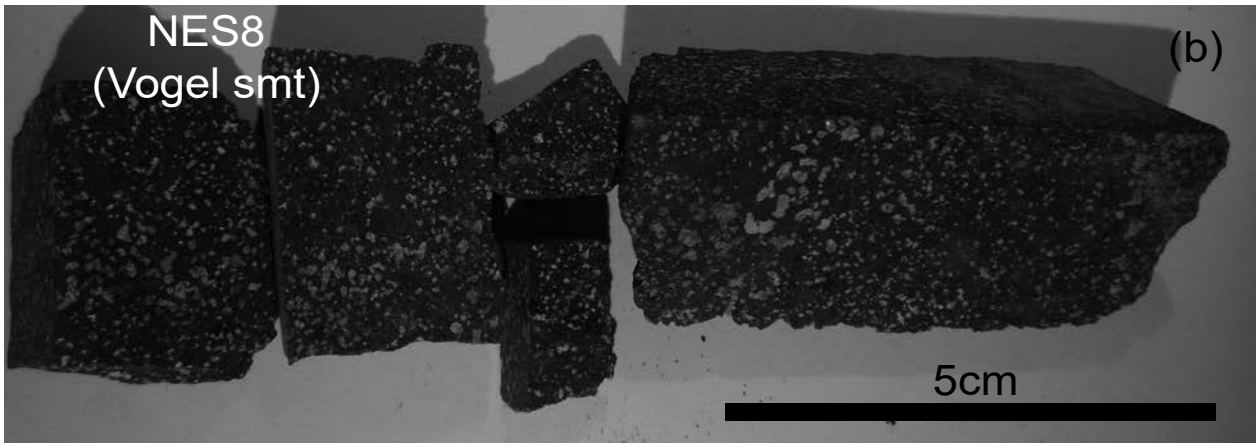
NES8
(Vogel smt)
(b)
5cm

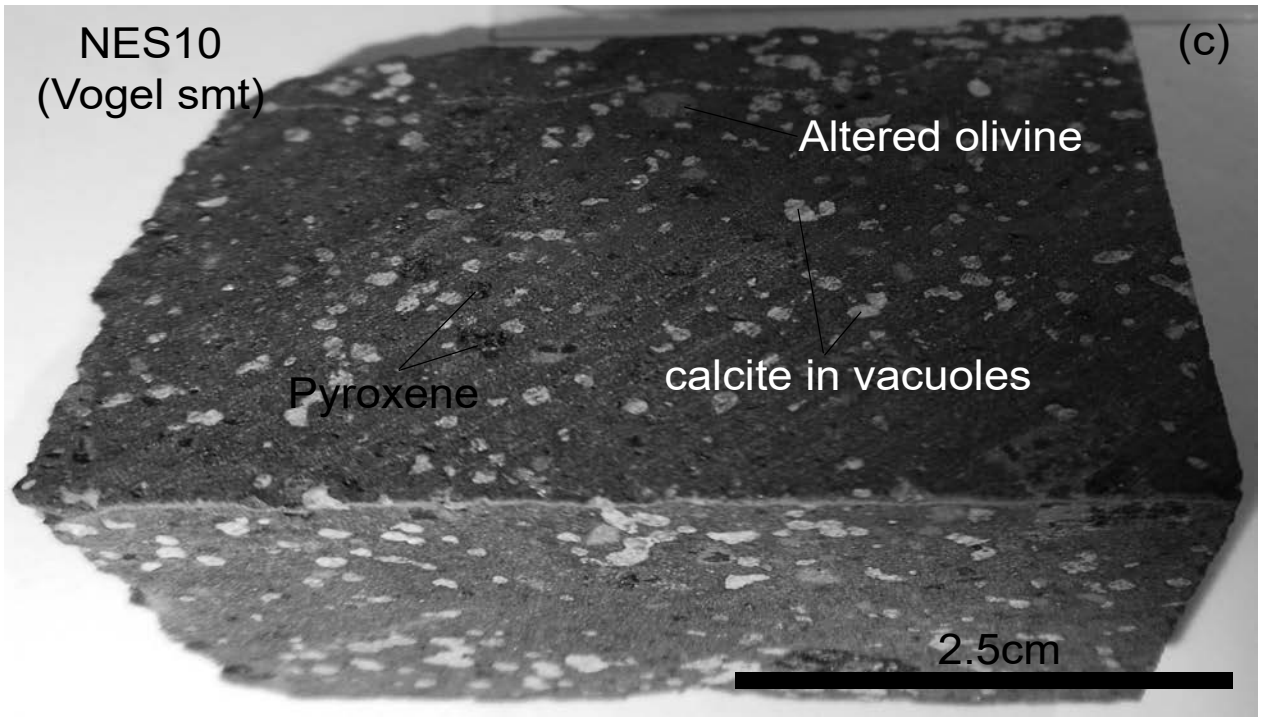
NES10
(Vogel smt)
(c)
Altered olivine
Pyroxene
calcite in vacuoles
2.5cm

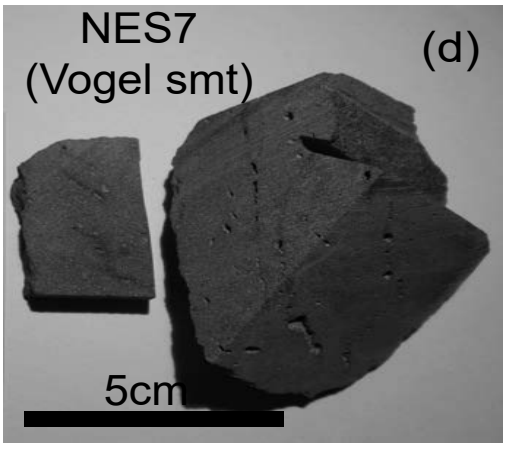
NES7
(Vogel smt)
(d)
5cm

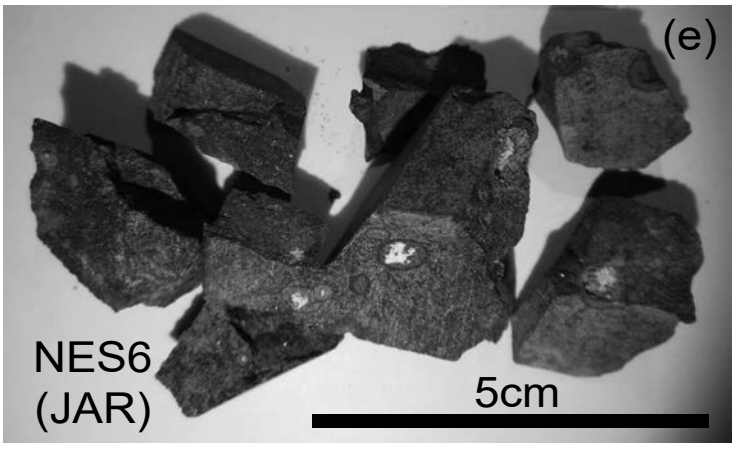
(e)
NES6
(JAR)
5cm

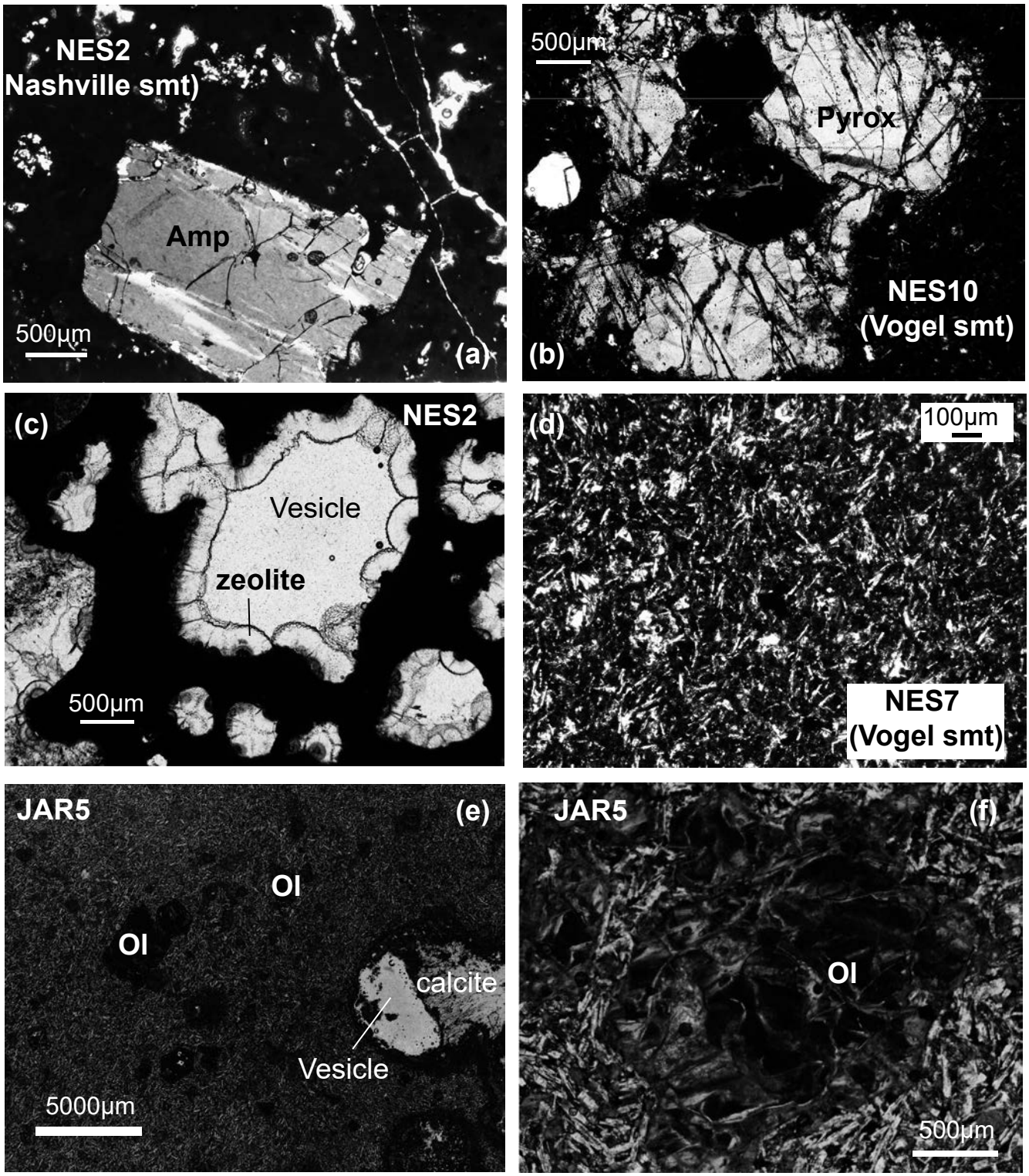
NES2
Nashville smt)
Amp
500µm
(a)
500µm
Pyrox
NES10
(Vogel smt)
(b)
(c)
NES2
Vesicle
zeolite
500µm
(d)
100µm
NES7
(Vogel smt)
JAR5
(e)
Ol
Ol
calcite
Vesicle
5000µm
JAR5
(f)
Ol
500µm

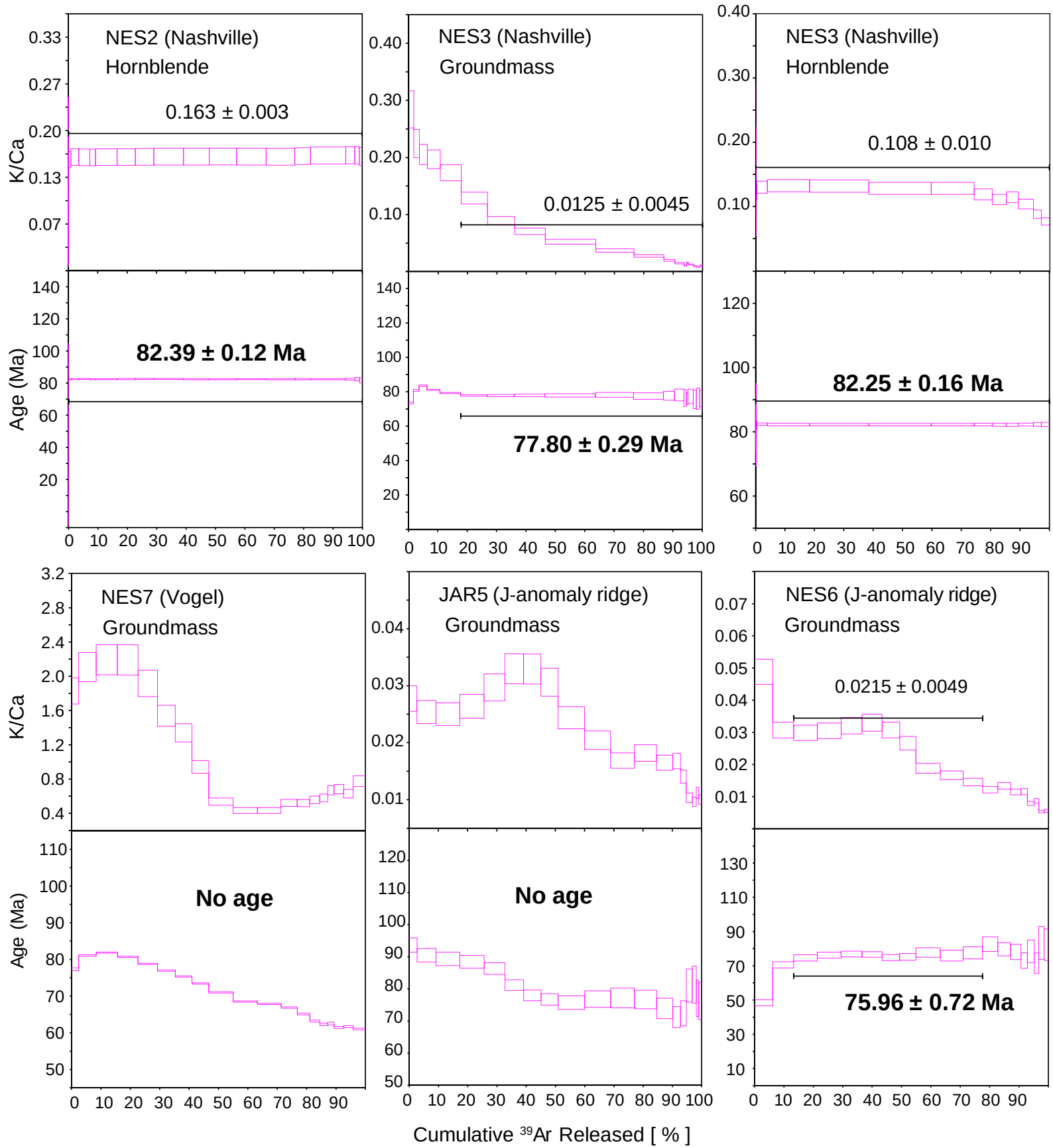
NES2 (Nashville)
Hornblende
0.163 ± 0.003
82.39 ± 0.12 Ma
NES3 (Nashville)
Groundmass
0.0125 ± 0.0045
77.80 ± 0.29 Ma
NES3 (Nashville)
Hornblende
0.108 ± 0.010
82.25 ± 0.16 Ma
NES7 (Vogel)
Groundmass
No age
JAR5 (J-anomaly ridge)
Groundmass
No age
NES6 (J-anomaly ridge)
Groundmass
0.0215 ± 0.0049
75.96 ± 0.72 Ma
K/Ca
Age (Ma)
Cumulative 39Ar Released [%]

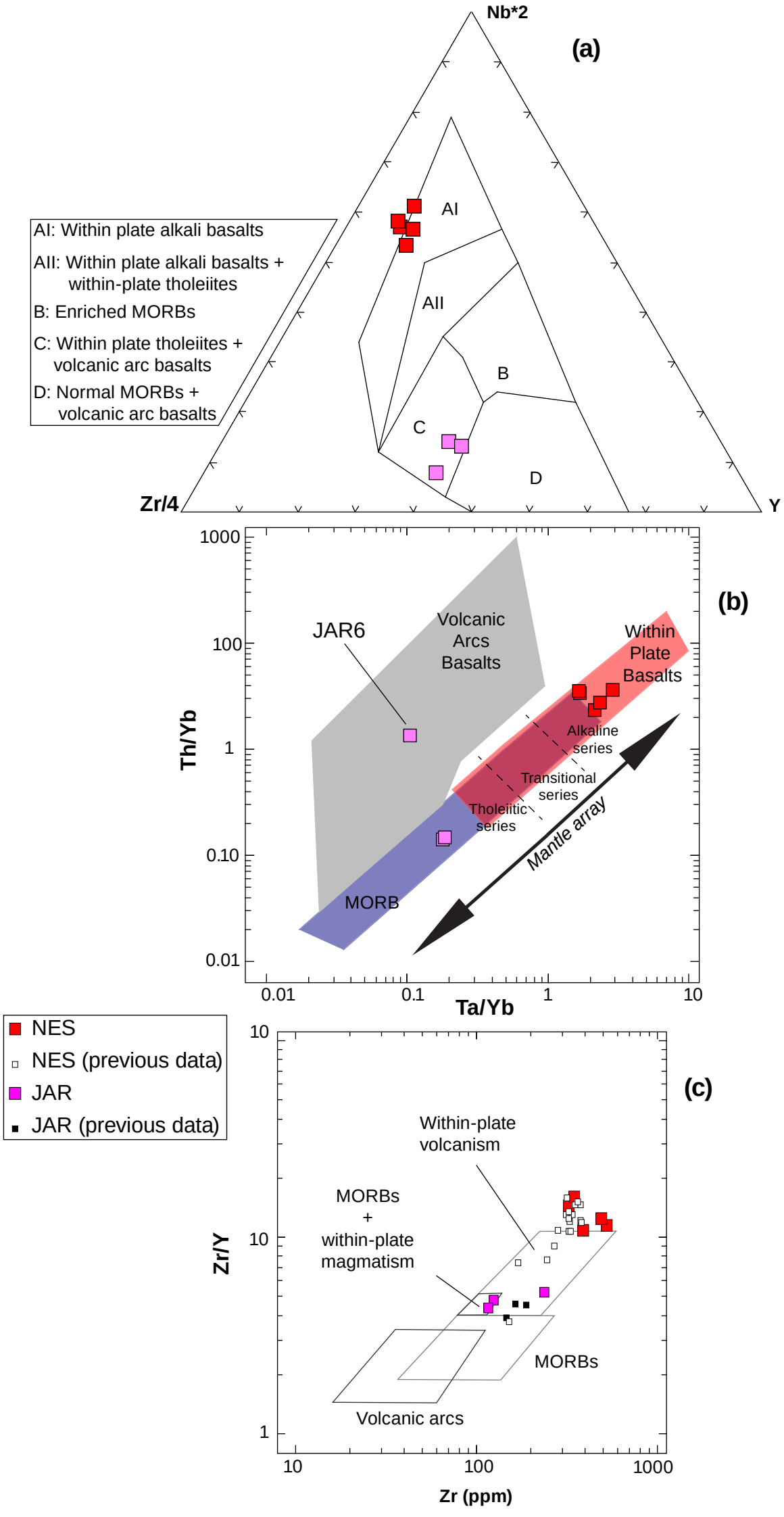
(a)
Nb*2
Zr/4
Y
AI: Within plate alkali basalts
AII: Within plate alkali basalts + within-plate tholeiites
B: Enriched MORBs
C: Within plate tholeiites + volcanic arc basalts
D: Normal MORBs + volcanic arc basalts
AI
AII
B
C
D
(b)
Th/Yb
Ta/Yb
JAR6
Volcanic Arcs Basalts
Within Plate Basalts
Alkaline series
Transitional series
Tholeiitic series
Mantle array
MORB
1000
100
1
0.10
0.01
0.01
0.1
1
10
NES
NES (previous data)
JAR
JAR (previous data)
(c)
Zr/Y
Zr (ppm)
Within-plate volcanism
MORBs + within-plate magmatism
MORBs
Volcanic arcs
10
10
1
10
100
1000

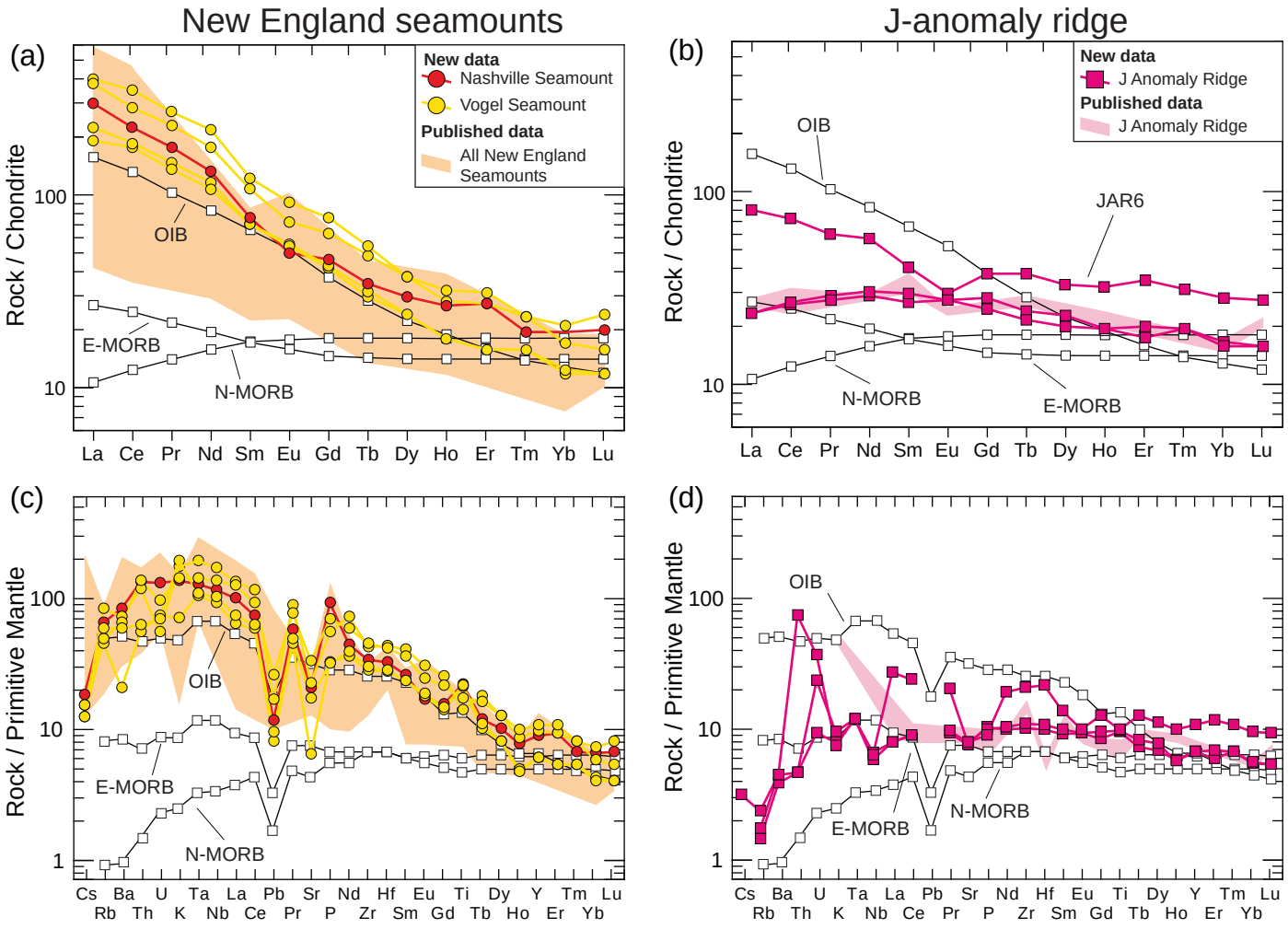

Merle et al., Figure XX

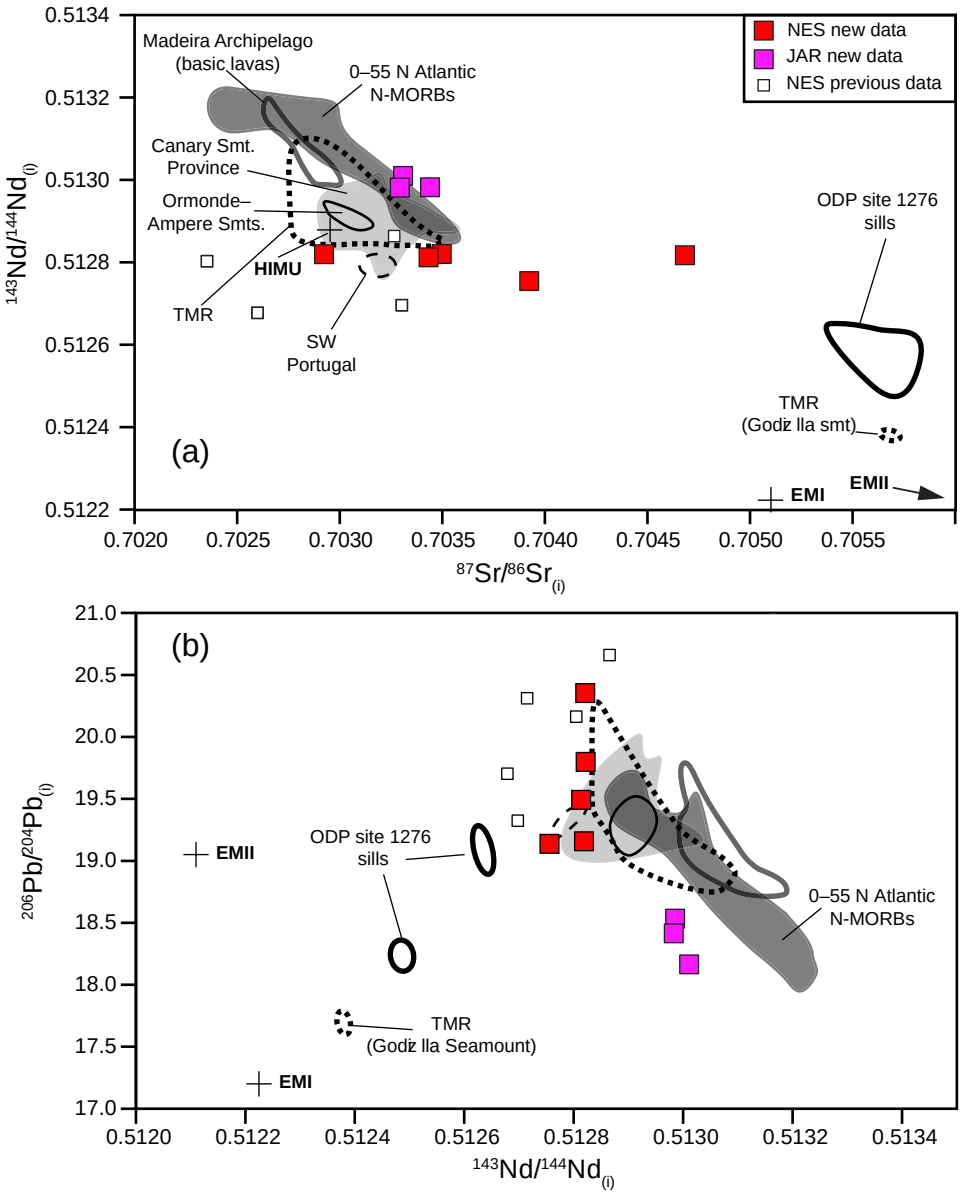

Merle et al., Figure 8

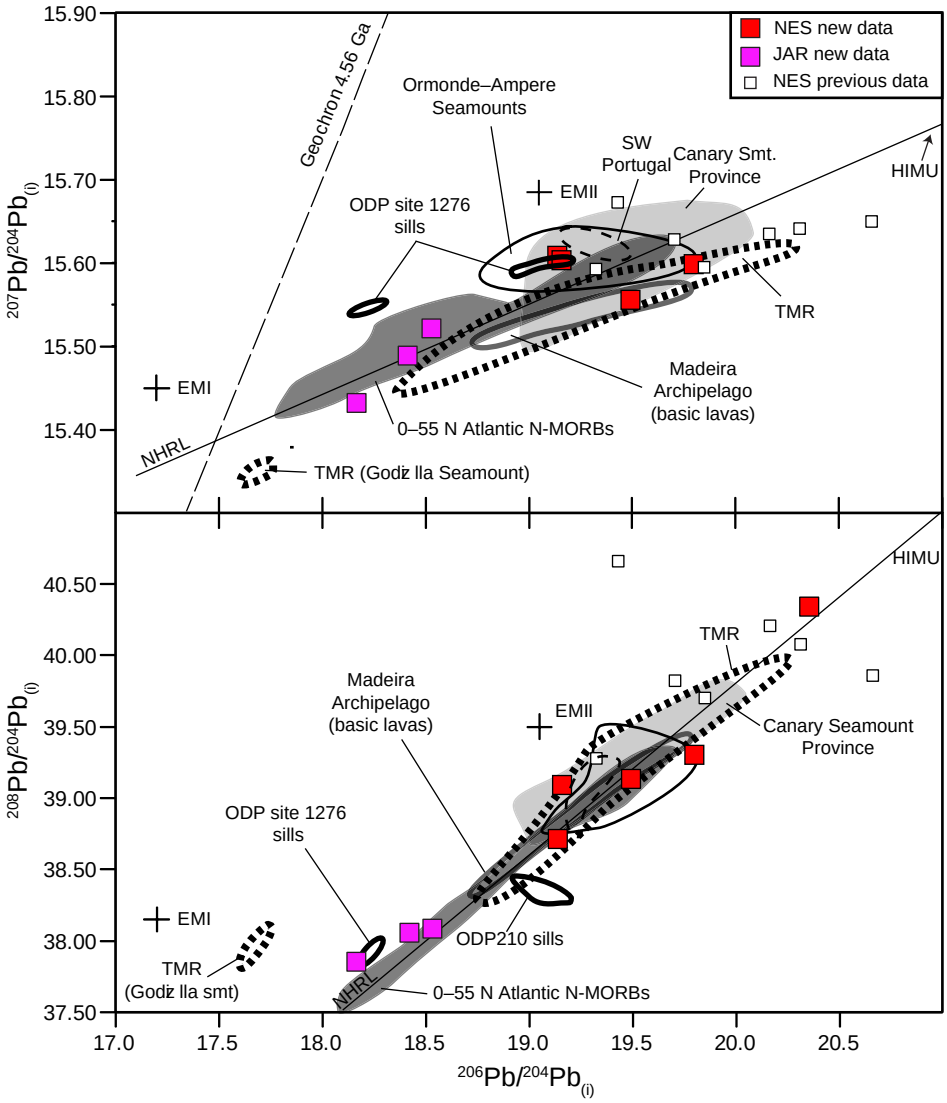

Merle et al., Figure 9

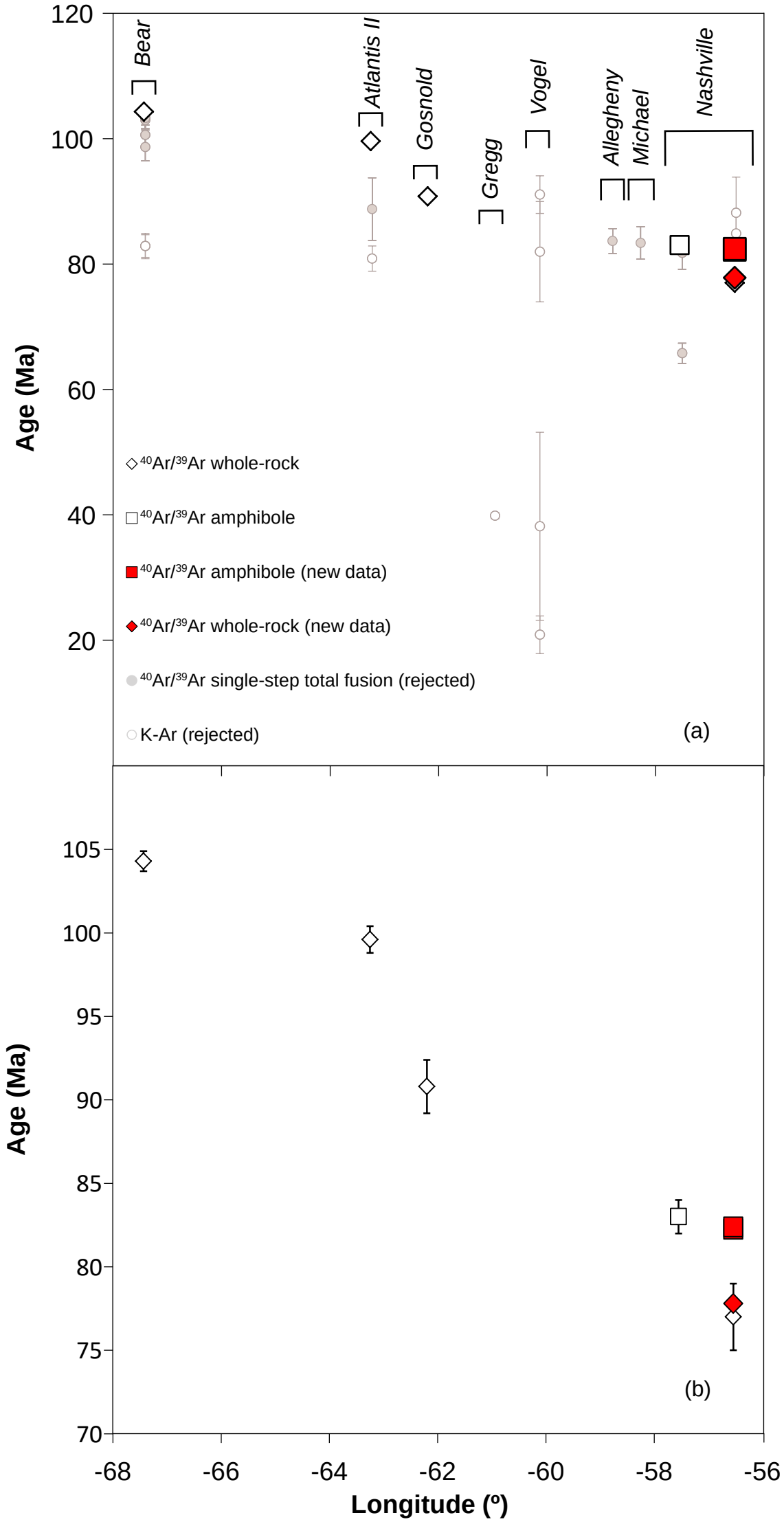
Bear
Atlantis II
Gosnold
Gregg
Vogel
Allegheny
Michael
Nashville
Age (Ma)
120
100
80
60
40
20
40Ar/39Ar whole-rock
40Ar/39Ar amphibole
40Ar/39Ar amphibole (new data)
40Ar/39Ar whole-rock (new data)
40Ar/39Ar single-step total fusion (rejected)
K-Ar (rejected)
(a)
Age (Ma)
105
100
95
90
85
80
75
70
(b)
-68
-66
-64
-62
-60
-58
-56
Longitude (º)

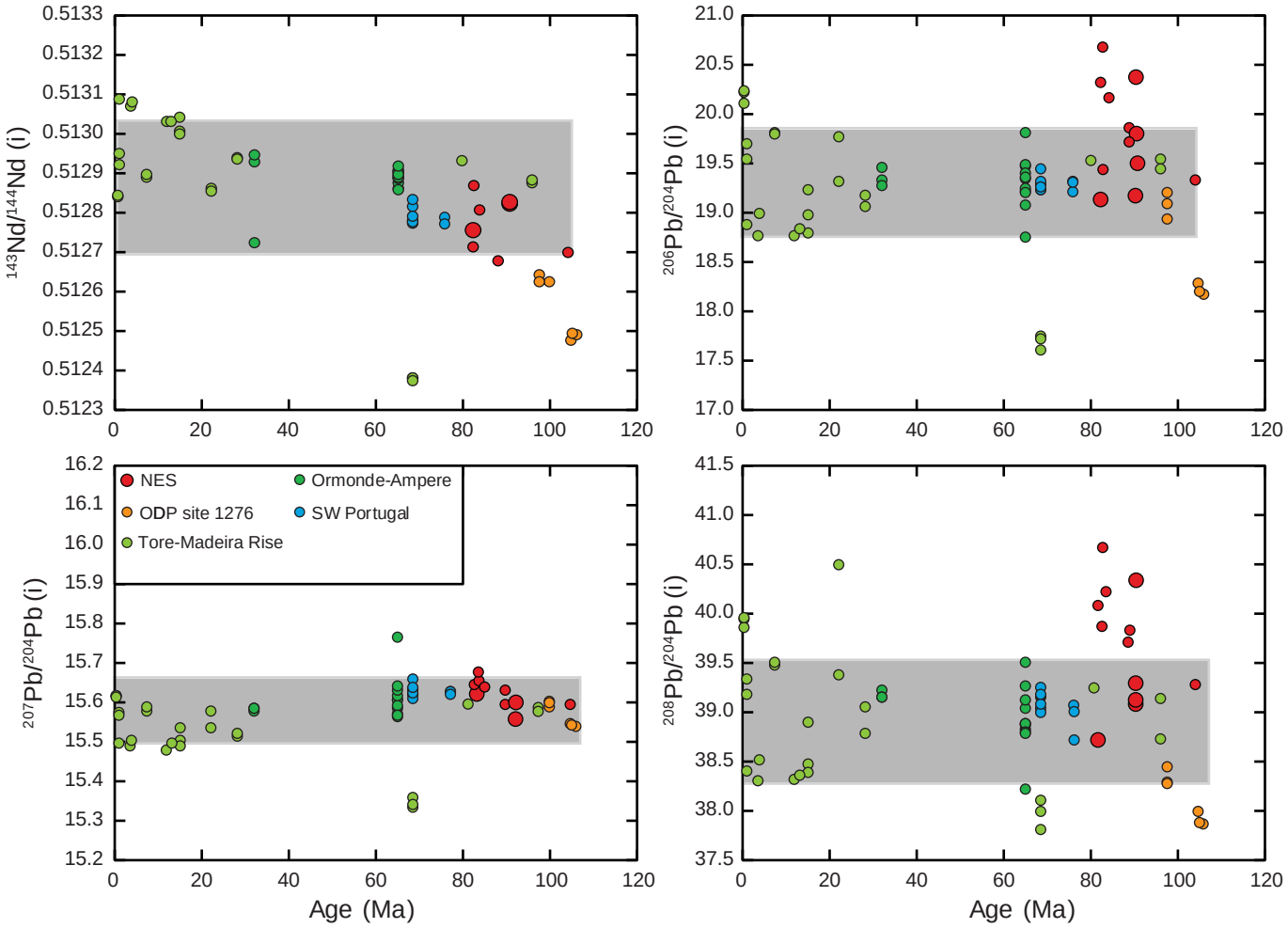

Merle et al., Figure 11

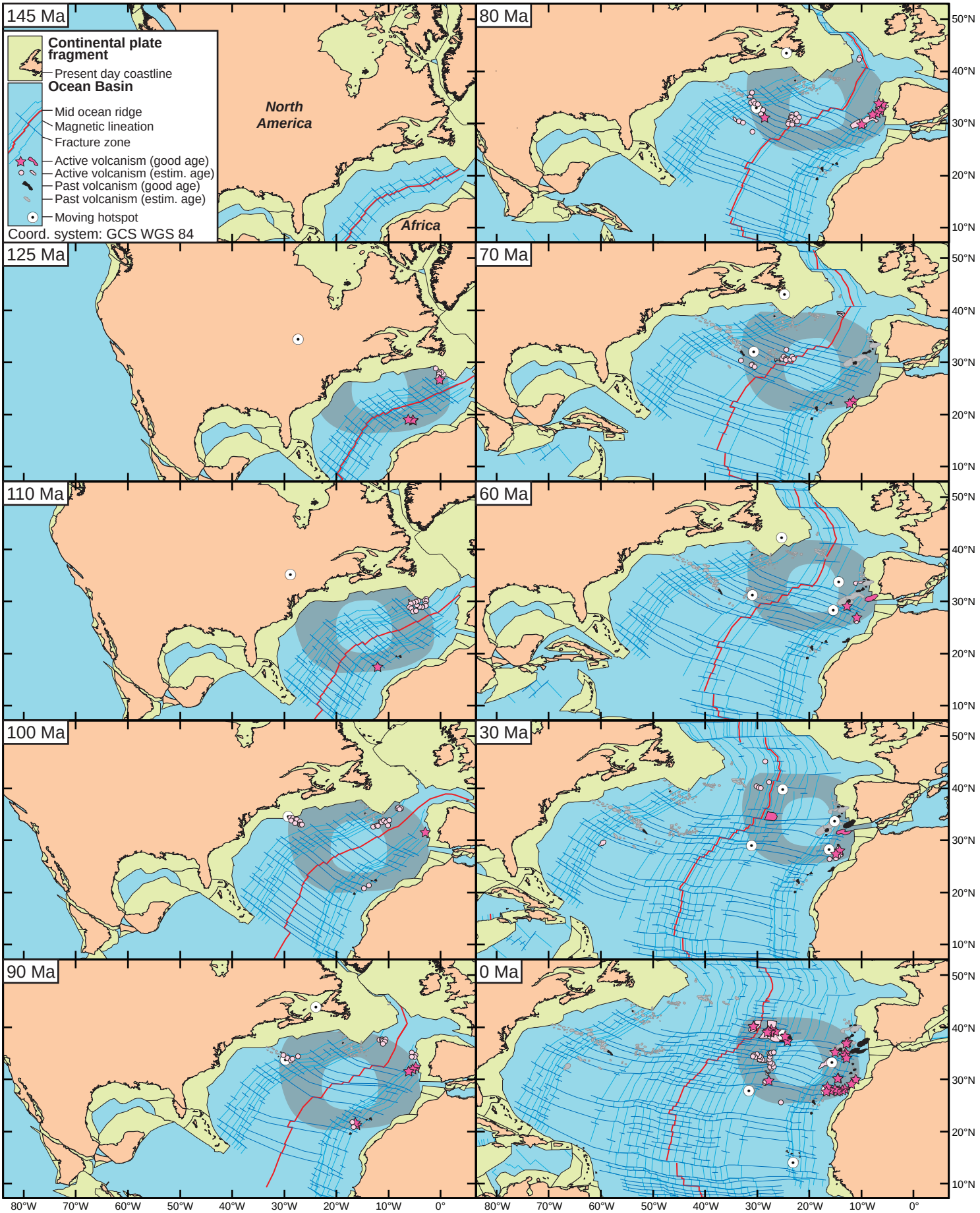

Merle et al., Figure 9

Table 1: Summary of $^{40}Ar/^{39}Ar$ dating

General characteristics			Plateau characteristics				Isochron characteristics					
Sample Name	**Dated material**	**K/Ca**	**Plateau Age (Ma ±2σ)**	**^{39}Ar Released (%)**	**MSWD**	**P**	**Inv. Isochron Age (Ma ±2σ)**	**n**	**$^{40}Ar/^{36}Ar$ Intercept (±2σ)**	**MSWD**	**P**	**Spreading factor (%)**
Nashville seamount (NES)												
NES 2	Hornblende	0.1630	82.39 ± 0.12	100	0.24	1	82.40 ± 0.14	17	296.6 ± 17.3	0.25	1	10
NES 3	Hornblende	0.1100	82.25 ± 0.16	100	0.70	0.81	82.24 ± 0.16	19	299.2 ± 1.2	0.7	0.8	91
NES 3	Groundmass	0.0100	77.80 ± 0.29	82	0.28	0.99	78.37 ± 0.82	14	288.8 ± 13.4	0.14	1	29.4
Vogel seamount (NES)												
NES 7	Groundmass	-	No plateau	-	-	-	-	-	-	-	-	-
J-anomaly ridge(JAR)												
NES 5	Groundmass	-	No plateau	-	-	-	-	-	-	-	-	-
NES 6	Groundmass	0.0220	75.96 ± 0.72	64	1.14	0.33	76.25 ± 3.37	9	297.4 ± 13.3	1.3	0.24	14.6

[a]MSWD and probability of fit (P) for plateau and isochron, percentage of ^{39}Ar degassed used in the plateau calculation, number of analyses included in the isochron, and $^{40}Ar/^{36}Ar$ intercept are indicated. Analytical uncertainties on the ages are quoted at 2 sigma (2σ) confidence levels.
*Samples with suffix -A are aliquots of the same sample prefix

Table 2: Sr-Nd isotopes data from NES and JAR basalts

location	Sample	$(^{87}Sr/^{86}Sr)_{meas}$	±2σ	$^{87}Rb/^{86}Sr$	$(^{87}Sr/^{86}Sr)_{ini}$	±2σ	$(^{143}Nd/^{144}Nd)_{meas}$	±2σ	$^{147}Sm/^{144}Nd$	$(^{143}Nd/^{144}Nd)_{ini}$	±2σ
Vogel	NES8	0.705492	0.000006	0.625442	0.704683	0.000006	0.512897	0.000002	0.129126	0.512820	0.000002
Vogel	NES10	0.703825	0.000005	0.302962	0.703433	0.000005	0.512885	0.000002	0.118919	0.512814	0.000002
Vogel	NES9	0.703664	0.000004	0.128372	0.703498	0.000004	0.512894	0.000002	0.119614	0.512823	0.000002
Vogel	NES7	0.703352	0.000005	0.331326	0.702923	0.000005	0.512889	0.000001	0.112874	0.512822	0.000001
Nashville	NES2	0.704245	0.000005	0.275704	0.703924	0.000005	0.512819	0.000002	0.115439	0.512757	0.000002
JAR	NES6	0.703327	0.000011	0.018791	0.703306	0.000011	0.513082	0.000003	0.140927	0.513012	0.000003
JAR	NES5	0.703466	0.000012	0.025459	0.703438	0.000012	0.513079	0.000003	0.190266	0.512985	0.000003
JAR	NES4	0.703309	0.000012	0.016207	0.703291	0.000012	0.513075	0.000003	0.183626	0.512984	0.000003

Table 3: Pb isotopes data from NES and JAR basalts

locality	Sample	$(^{206}Pb/^{204}Pb)_{meas}$	±2σ	$^{238}U/^{204}Pb$	$(^{207}Pb/^{204}Pb)_{meas}$	±2σ	$^{235}U/^{204}Pb$	$(^{208}Pb/^{204}Pb)_{meas}$	±2σ	$^{232}Th/^{204}Pb$	$(^{206}Pb/^{204}Pb)_{ini}$	±2σ	$(^{207}Pb/^{204}Pb)_{ini}$	±2σ	$(^{208}Pb/^{204}Pb)_{ini}$	±2σ
Vogel	NES8	20.159	0.0040	69.77	15.650	0.003	0.51	40.087	0.008	220.81	19.164	0.004	15.602	0.0032	39.090	0.008
Vogel	NES10	20.276	0.0072	54.54	15.592	0.005	0.40	40.066	0.014	206.64	19.498	0.0072	15.555	0.0055	39.133	0.014
Vogel	NES9	20.205	0.0049	28.03	15.617	0.003	0.21	40.061	0.008	168.27	19.805	0.0049	15.597	0.0029	39.302	0.008
Vogel	NES7	20.721	0.0061	25.27	16.112	0.005	0.19	41.373	0.012	228.46	20.361	0.0061	16.095	0.0049	40.342	0.0124
Nashville	NES2	20.253	0.0063	86.46	15.661	0.005	0.64	40.190	0.012	363.54	19.144	0.0063	15.608	0.0048	38.713	0.0124
JAR	NES6	18.165	0.0213	-	15.432	0.018	-	37.861	0.045	-	-	-	-	-	-	-
JAR	NES5	18.528	0.0177	-	15.522	0.015	-	38.094	0.036	-	-	-	-	-	-	-
JAR	NES4	18.418	0.0161	-	15.489	0.013	-	38.058	0.032	-	-	-	-	-	-	-